

CHAPTER 4

RESULTS

4.1 *Pediastrum* spp. diversity

A total of 26 species of *Pediastrum* consisting of 60 taxa were obtained from 68 sampling sites. *P. duplex* was the most widely distributed species with 20% (12 taxa) of the total *Pediastrum* population followed by *P. boryanum* and *P. simplex* with 13.3% (8 taxa), *P. tetras* (6.7%, 4 taxa), *P. biradiatum* (5.0%, 3 taxa), *P. angulosum*, *P. araneosum*, *P. clathratum*, *P. integrum* (3.3%, 2 taxa) and 17 remaining species were found in smaller number (1.7%, 1 taxa) such as *P. alternans*, *P. argentinense*, *P. asymmetricum*, *P. biwae*, *P. braunii*, *P. emarginatum*, *P. kawraiskyi*, *P. longicornutum*, *P. muticum*, *P. obtusum*, *P. orbitale*, *P. pertusum*, *P. privum*, *P. sculptatum*, *Pediastrum* sp. 1, *Pediastrum* sp. 2, *Pediastrum* sp. 3 (Figure 5). They were classified systematically into categories as shown in Table 3. *Pediastrum* spp. could be found in oligo-mesotrophic, mesotrophic, meso-eutrophic and eutrophic statuses. They were most abundant in the meso-eutrophic followed by mesotrophic, oligo-mesotrophic and eutrophic statuses. The most abundant species; *P. duplex* var. *duplex* Meyen, *P. tetras* (Ehrenberg) Ralfs and *P. simplex* var. *simplex* Meyen were found in all trophic statuses (Table 4). All taxa were documented using light microscope. However, light microscopic

method alone is laborious, often unsuccessful in identifying relatively small cells without distinctive morphological characteristics. They were documented using SEM which can visualize details of the cell wall clearly. The types of cell wall sculptures together with morphological modifications in the coenobium are diagnostic features for different taxa at species or variety levels. For examples cell wall is net like with warts: *P. alternans* Nygaard, *P. boryanum* (Turpin) var. *boryanum* Meneghinias, *P. boryanum* var. *longicorne* Reinsch and *P. subgranulosum* Raciborski. Cell wall is net like: *P. duplex* var. *asperum* A. Braun, *P. duplex* var. *gracillimum* West & G.S.West, *P. tetras* var. *tetraodon* (Corda) Hansgirg and *P. privum* (Printz) E.Hegewald. Cell wall is warty (large conical warts): *P. simplex* var. *echinulatum* Wittrock Cell wall is wrinkled: *P. simplex* var. *simplex* Meyen and *P. tetras* var. *excisum* Rabenhorst. Cell wall is warty (dense rounded warts): *P. simplex* var. *sturmii* (Reinsch) Wolle and *P. biwae* Negoro. Cell wall is smooth: *P. duplex* var. *duplex* Meyen, *P. longicornutum* Gutwinski and *P. biradiatum* var. *glabrum* (Raciborski) Parra and cell wall is papillose: *P. asymmetricum* T.Yamagishi & E.Hegewald which. The light and SEM pictures of *Pediastrum* species are shown in Figures 6-12.

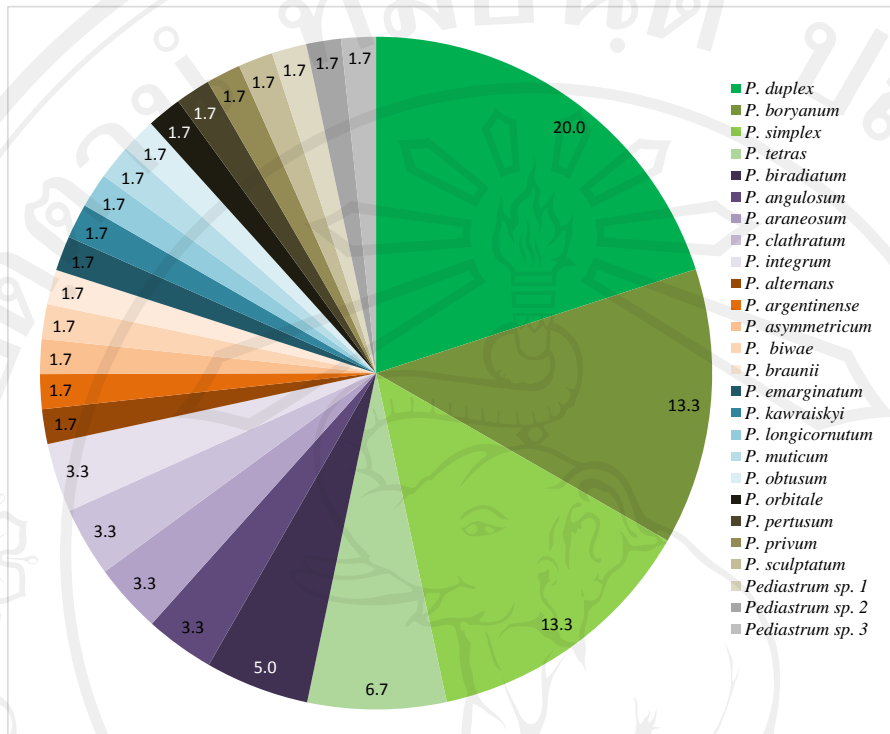


Figure 5 Percentage of *Pediastrum* species from 68 sampling sites

4.2 New record of *Pediastrum* species in Thailand

A total of 22 taxa of *Pediastrum* spp. were revealed to be new record for Thailand (Figure13). They were compared with the checklist of freshwater algae and publications of Thailand (West and West, 1902; Hirano, 1967; Hirano, 1975; Lewmanomont *et al.*, 1995 and Peerapornpisal, 1996). The new record species are indicated by symbol (*) after the species name in Table 3.

Table 3 List of *Pediastrum* spp. and occurrence at 68 sampling sites (Occurrence: + rare, ++ = occasional, +++ = frequent and *= new record)

Species	Occurrence	Locations
<i>Pediastrum alternans</i> Nygaard*	+	NPN2
<i>P. angulosum</i> Ehrenberg ex Meneghini*	++	NST2, SKA1
<i>P. angulosum</i> var. <i>coronatum</i> (Raciborski)* J.Komárek & V.Jankovská	++	KKN2, SSK1
<i>P. araneosum</i> (Raciborski) Raciborski	++	NPT1, CTB1
<i>P. araneosum</i> var. <i>rugulosum</i> G.S.West	++	CHM1, UBR1
<i>P. argentinense</i> Bourrelly & Tell	++	UTT1, PTL1
<i>P. asymmetricum</i> T.Yamagishi & E.Hegewald*	+	PCB1
<i>P. biradiatum</i> Meyen	+++	CHM1, CHM3, PNS1, SSK1, PTL1, SKA1,
<i>P. biradiatum</i> var. <i>emarginatum</i> (Ehrenberg) Lagerheim	+++	CHM3, PNS1, LOE1, RET2
<i>P. biradiatum</i> var. <i>glabrum</i> (Raciborski) Parra*	+++	CHM3, PNS1, SBR1, LOE1, SRT2, PTL1,
<i>P. biwae</i> Negoro*	+++	CHM3, NKS2, UTT1, RET2, KKN1, KCN1, KCN2, PBR1, NRS2, RYN1, NKS1
<i>P. boryanum</i> (Turpin) var. <i>boryanum</i> Meneghini	+++	CHR1, CHM1, CHM2, CHM3, PHR1, UTD1, PSL1, NKS2, PHC1, PNS1, ANT1, SBR1, SPB1, UTT1, NPT1, KLS1, SUR1, , SSK1, CCS1, RYN2, CTB1, TAK1, SRT1, NST1
<i>P. boryanum</i> var. <i>brevicorne</i> Braun	++	CHM3, PBR1
<i>P. boryanum</i> var. <i>caribbeanum</i> A.Comas*	++	CHM3, SPB1, RYN1
<i>P. boryanum</i> var. <i>cornutum</i> (Raciborski) Sulek	+++	CHM2, ANT1, SBR1, CHP1, SRT1
<i>P. boryanum</i> var. <i>forcipatum</i> (Corda) Chodat*	++	CHM3, SKT1, PHC1
<i>P. boryanum</i> var. <i>longicorne</i> Reinsch*	++	RET2, NRS2, RYN1
<i>P. boryanum</i> var. <i>perforatum</i> (Raciborski) Nitardy*	++	CHM3, LOE1
<i>P. boryanum</i> var. <i>pseudoglabrum</i> Parra* Barrientos	++	CHM3, NRS2
<i>P. braunii</i> Waetm. Schweiz	++	NPN2, KLS1, STN1
<i>P. clathratum</i> (Schröder) Lemmermann	++	PSL1, RYN1
<i>P. clathratum</i> var. <i>radians</i> (Lemmermann) Bachmann	++	CHP1, SKT1

Table 3 (Continued)

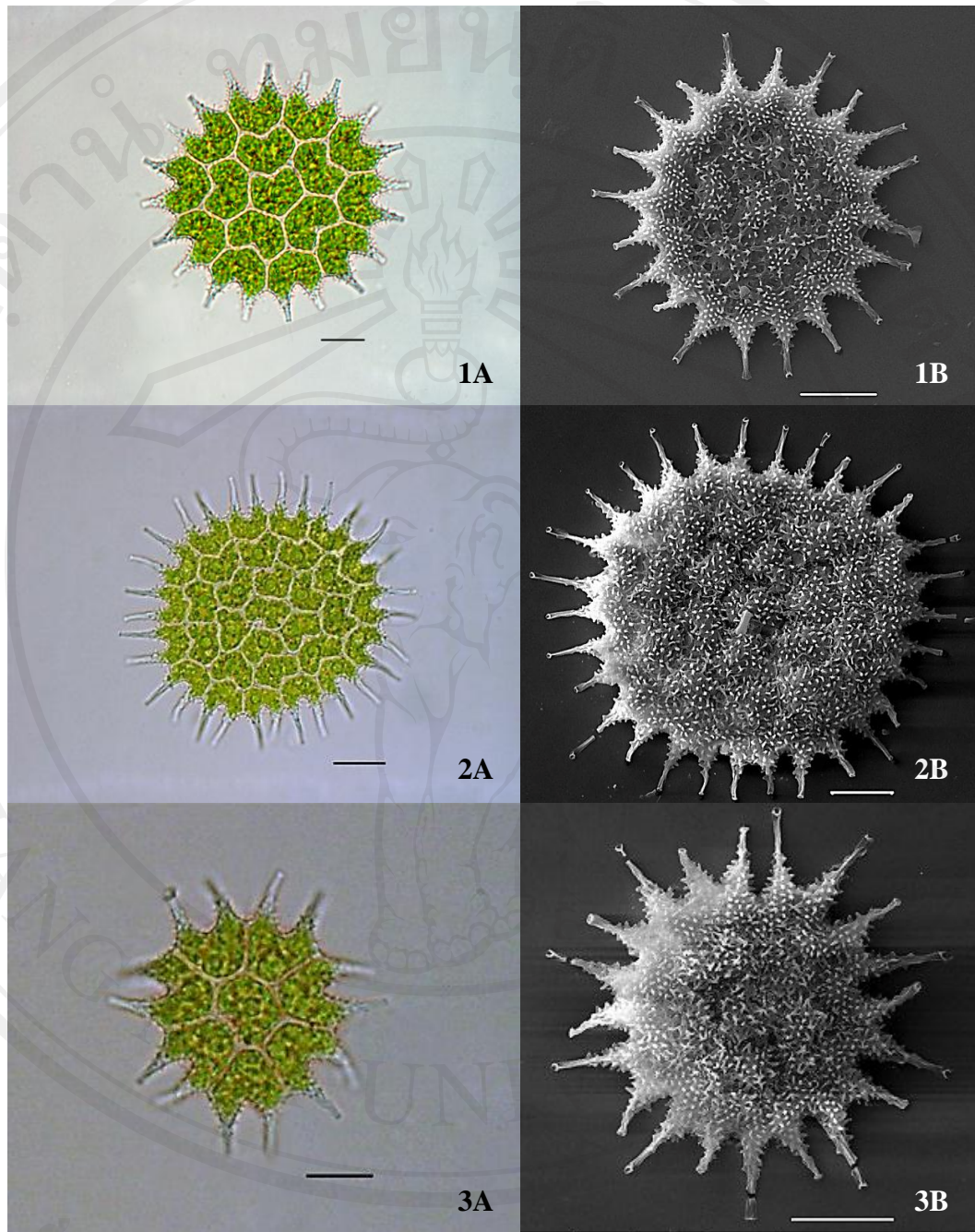
Species	Occurrence	Locations
<i>P. duplex</i> var. <i>duplex</i> Meyen	++++	CHR1, CHM1, CHM2, CHM3, PHR1, UTD1, PSL1, NKS2, PHC1, PNS1, ANT1, SBR1, SPB1, UTT1, NPT1, KLS1, SUR1, SUR2, SSK1,
<i>P. duplex</i> var. <i>asperum</i> A. Braun*	+++	PHY2, UTD1, PHC1, ANT1, SPB1, UTT1, SUR1, CCS1, RYN1, CTB2, KCN1, NST1, PTL1
<i>P. duplex</i> var. <i>clathralum</i> (A. Braun) Lagerheim	++	CHR1, PBR1
<i>P. duplex</i> var. <i>cohaerens</i> (Bohlin) Ergashev	++	CHR1, PSL1
<i>P. duplex</i> var. <i>cornutum</i> J. Komárek & V. Jankovská	++	UTT1, SRT1, NST3
<i>P. duplex</i> var. <i>coronatum</i> Raciborski*	++	CHM3, RYN1, PTL1
<i>P. duplex</i> var. <i>genuinum</i> (A. Braun) Lagerheim*	++	UTD1, RYN2
<i>P. duplex</i> var. <i>gracillimum</i> West & G.S. West	+++	CHM1, CHM3, UTD1, PSL1, UTT2, SUR1, UBR1, CCS1, CTB1, SRT1, PTL1, STN1
<i>P. duplex</i> var. <i>punctatum</i> (Willi Krieger) Parra	++	PSL1, NPT1
<i>P. duplex</i> var. <i>reticulatum</i> Lagerheim	++	PHR1, ANT1
<i>P. duplex</i> var. <i>rotundatum</i> Lucks	++	CHR1, SRB1
<i>P. duplex</i> var. <i>rugulosum</i> Raciborski	++	CHM3, UTD1, SUR1, RYN1, KCN1
<i>P. emarginatum</i> Kützing	++	CHM3, PTL1
<i>P. integrum</i> Nägeli	++	SRT2, PTL1
<i>P. integrum</i> var. <i>perforatum</i> Raciborski*	++	CTB1, SRT1
<i>P. kawraiskyi</i> Schmidle*	++	CHR1, SKA1
<i>P. longicornutum</i> Gutwinski	+++	CHM3, PNS1, SBR1, SUR2
<i>P. muticum</i> Kützing*	++	PHR1, NST1
<i>P. obtusum</i> Lucks	++	CTB1, SRT1
<i>P. orbitale</i> Komarek	++	PHY2, PSL1
<i>P. pertusum</i> Kützing*	++	CHR1, CHM3
<i>P. privum</i> (Printz) E. Hegewald	+	CHM3
<i>P. simplex</i> var. <i>simplex</i> Meyen	++++	CHR1, CHM1, CHM2, CHM3, PHY2, SKT1, PSL1, NKS1, NKS2, PCB2, SRB1, SBR1, SPB1, PTT, UTT1, NPT1, NPT2, LOE1, MDH1, YST1,

Table 3 (Continued)

Species	Occurrence	Locations
<i>P. simplex</i> var. <i>clathratum</i> Schröter	+++	RET2, KLS1, NRS1, NRS2, SSK2, CCS1, CTB1, SKO1, SRT2, SRT3, NST3 CHR1, SKT1, NKS1, NKS2, PCB1, SRB1, UTT1, LOE1, UDT1, NRS1, CTB1, KCN1, KCN2, RBR1, SRT2
<i>P. simplex</i> var. <i>duodenarium</i> (J.W.Bailey) Rabenhorst	++	CHM3, PHY2, PCB2, PTT
<i>P. simplex</i> var. <i>echinulatum</i> Wittrock	+++	CHM3, PHY1, NKS1, PCB2, PTT1, SPB1, UTT1, LOE1, NKI1, RET2, KLS1, KKN2, SSK2, CCS1, KCN1, KCN2, RBR1, PBR1, SRT2, SRT3, NST1
<i>P. simplex</i> var. <i>granulatum</i> Lemmermann	++	CHM3, PHY2
<i>P. simplex</i> var. <i>pseudoglabrum</i> Parra Barrientos*	+++	CHM3, SKT1, NKS2, PTT1, UTT1, KKN1, SKO1, SRT2, NST3
<i>P. simplex</i> var. <i>radians</i> Lemmermann	++	CHR1, RET2
<i>P. simplex</i> var. <i>sturmii</i> (Reinsch) Wolle	+++	CHM3, PHY2, NKS1, NKS2, PCB1, NKI1, SRT2
<i>P. subgranulosum</i> Raciborski*	+++	CHM3, ANT1, LOE1, RYN1, KCN1, PTL1
<i>P. tetras</i> (Ehrenberg) Ralfs	++++	CHR1, CHM1, CHM2, CHM3, PHC1, SPB1, UTT1, UTT2, LOE1, UDT1, NPN2, MDH1, RET2, KLS1, NRS2, KKN2, SUR2, SSK1, SSK2, UBR1, CCS1, KCN3, CBR1, RYN1, TAK1, SRT1, NST1, NST2, PTL1, SKA1, STN1
<i>P. tetras</i> var. <i>apiculatum</i> Playfair*	++	CHM3, LOE1, CBR1
<i>P. tetras</i> var. <i>excisum</i> Rabenhorst*	+++	CHM3, SPB1, UTT1, UTT2, UBR1, NST1, NST3, PTL1,
<i>P. tetras</i> var. <i>tetraodon</i> (Corda) Hansgirg	+++	CHM3, UTT1, LOE1, NPN1, SUR2, SSK1, CBR1, TAK1, SRT1, PTL1
<i>P. sculptatum</i> G.M.Smith	++	CHR1, PHC1
<i>Pediastrum</i> sp. 1	++	CHR1, RET1
<i>Pediastrum</i> sp. 2	++	LOE1, NPN1, UBR1, SRT2
<i>Pediastrum</i> sp. 3	++	CHM3, LOE1, CBR1

Table 4 Distribution of *Pediastrum* species in each trophic status

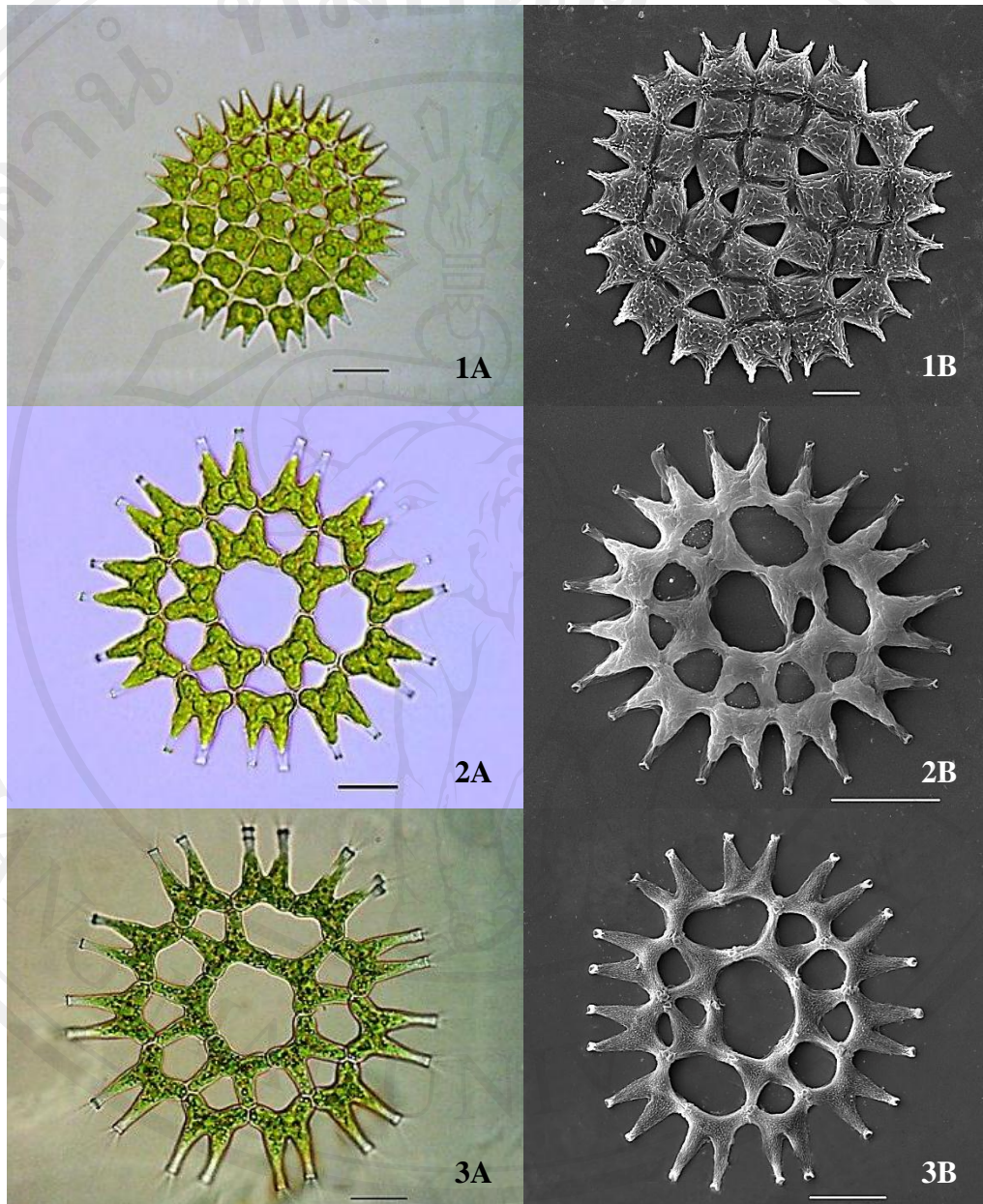
Trophic status	Species occurring		
Oligo-mesotrophic	<i>P. alternans</i> Nygaard, <i>P. biradiatum</i> Meyen, <i>P. duplex</i> var. <i>duplex</i> Meyen, <i>P. simplex</i> var. <i>echinulatum</i> Wittrock,	<i>P. angulosum</i> Ehrenberg ex Meneghini, <i>P. boryanum</i> (Turpin) var. <i>boryanum</i> Meneghini, <i>P. duplex</i> var. <i>gracillimum</i> West & G.S.West, <i>P. tetras</i> (Ehrenberg) Ralfs	<i>P. angulosum</i> var. <i>coronatum</i> (Raciborski) J.Komárek & V.Jankovská, <i>P. braunii</i> Waetm. Schweiz, <i>P. simplex</i> var. <i>simplex</i> Meyen,
Mesotrophic	<i>P. araneosum</i> (Raciborski) Raciborski, <i>P. biwae</i> Negoro, <i>P. boryanum</i> var. <i>forcipatum</i> (Corda) Chodat, <i>P. duplex</i> var. <i>asperum</i> A. Braun, <i>P. duplex</i> var. <i>reticulatum</i> Lagerheim, <i>P. obtusum</i> Lucks, <i>P. simplex</i> var. <i>duodenarium</i> (J.W.Bailey) Rabenhorst, <i>P. simplex</i> var. <i>sturmii</i> (Reinsch) Wolle, <i>Pediastrum</i> sp. 3	<i>P. araneosum</i> var. <i>rugulosum</i> G.S.West, <i>P. boryanum</i> (Turpin) var. <i>boryanum</i> Meneghini, <i>P. clathratum</i> var. <i>radians</i> (Lemmermann) Bachmann, <i>P. duplex</i> var. <i>cornutum</i> J.Komárek & V. Jankovská, <i>P. integrum</i> var. <i>perforatum</i> Raciborski, <i>P. simplex</i> var. <i>simplex</i> Meyen, <i>P. simplex</i> var. <i>echinulatum</i> Wittrock, <i>P. tetras</i> (Ehrenberg) Ralfs,	<i>P. argentinense</i> Bourrelly & Tell, <i>P. boryanum</i> var. <i>cornutum</i> (Raciborski) Sulek, <i>P. duplex</i> var. <i>duplex</i> Meyen, <i>P. duplex</i> var. <i>gracillimum</i> West & G.S.West, <i>P. muticum</i> Kützing, <i>P. simplex</i> var. <i>clathratum</i> Schröter, <i>P. simplex</i> var. <i>pseudoglabrum</i> Parra Barrientos, <i>P. tetras</i> var. <i>tetraodon</i> (Corda) Hansgirg,
Meso-eutrophic	<i>P. araneosum</i> (Raciborski) Raciborski, <i>P. asymmetricum</i> T.Yamagishi & E.Hegewald, <i>P. biradiatum</i> var. <i>glabrum</i> (Raciborski) Parra, <i>P. boryanum</i> var. <i>brevicorne</i> Braun, <i>P. boryanum</i> var. <i>forcipatum</i> (Corda) Chodat, Nitardy, <i>P. boryanum</i> var. <i>pseudoglabrum</i> Parra Barrientos*, <i>P. duplex</i> var. <i>asperum</i> A. Braun, <i>P. duplex</i> var. <i>coronatum</i> Raciborski, <i>P. duplex</i> var. <i>reticulatum</i> Lagerheim, <i>P. emarginatum</i> Kützing, <i>P. longicornutum</i> Gutwinski, <i>P. privum</i> (Printz) E.Hegewald, <i>P. simplex</i> var. <i>duodenarium</i> (J.W.Bailey) Rabenhorst, <i>P. simplex</i> var. <i>radians</i> Lemmermann, <i>P. tetras</i> (Ehrenberg) Ralfs, <i>P. sculptatum</i> G.M.Smith, <i>Pediastrum</i> sp. 1,	<i>P. araneosum</i> var. <i>rugulosum</i> G.S.West, <i>P. biradiatum</i> Meyen, <i>P. biwae</i> Negoro, <i>P. boryanum</i> var. <i>caribbeanum</i> A.Comas, <i>P. boryanum</i> var. <i>longicorne</i> Reinsch, <i>P. clathratum</i> var. <i>radians</i> (Lemmermann) Bachmann, <i>P. duplex</i> var. <i>clathralum</i> (A. Braun) Lagerheim, <i>P. duplex</i> var. <i>gracillimum</i> West & G.S.West, <i>P. duplex</i> var. <i>rotundatum</i> Lucks, <i>P. integrum</i> Nägeli, <i>P. orbitale</i> Komarek, <i>P. simplex</i> var. <i>simplex</i> Meyen, <i>P. simplex</i> var. <i>echinulatum</i> Wittrock, <i>P. simplex</i> var. <i>granulatum</i> Lemmermann, <i>P. simplex</i> var. <i>sturmii</i> (Reinsch) Wolle, <i>P. tetras</i> var. <i>apiculatum</i> Playfair, <i>Pediastrum</i> sp. 2,	<i>P. argentinense</i> Bourrelly & Tell, <i>P. biradiatum</i> var. <i>emarginatum</i> (Ehrenberg) Lagerheim, <i>P. boryanum</i> (Turpin) var. <i>boryanum</i> Meneghini, <i>P. boryanum</i> var. <i>cornutum</i> (Raciborski) Sulek, <i>P. boryanum</i> var. <i>perforatum</i> (Raciborski)*, <i>P. duplex</i> var. <i>duplex</i> Meyen, <i>P. duplex</i> var. <i>cohaerens</i> (Bohlin) Ergashev, <i>P. duplex</i> var. <i>punctatum</i> (Willi) Krieger Parra, <i>P. duplex</i> var. <i>rugulosum</i> Raciborski, <i>P. kawraiskyi</i> Schmidle, <i>P. pertusum</i> Kützing, <i>P. simplex</i> var. <i>clathratum</i> Schröter, <i>P. simplex</i> var. <i>pseudoglabrum</i> Parra Barrientos, <i>P. subgranulosum</i> Raciborski, <i>P. tetras</i> var. <i>tetraodon</i> (Corda) Hansgirg, <i>Pediastrum</i> sp. 3
Eutrophic	<i>P. boryanum</i> (Turpin) var. <i>boryanum</i> Meneghini, <i>P. tetras</i> (Ehrenberg) Ralfs Lagerheim, <i>P. simplex</i> var. <i>simplex</i> Meyen	<i>P. duplex</i> var. <i>duplex</i> Meyen, <i>P. duplex</i> var. <i>gracillimum</i> West & G.S.West,	<i>P. duplex</i> var. <i>genuinum</i> (A.Braun), <i>P. duplex</i> var. <i>rugulosum</i> Raciborski,
Hypereutrophic	absent		



scale bar 10 μm

Figure 6 1A-3A; Light micrographs and 1B-3B; scanning electron micrographs of *Pediastrum* spp.

1A, 1B *P. boryanum* (Turpin) var. *boryanum* Meneghini, 2A, 2B *P. boryanum* var. *longicorne* Reinsch, 3A, 3B *P. boryanum* var. *pseudoglabrum* Parra Barrientos

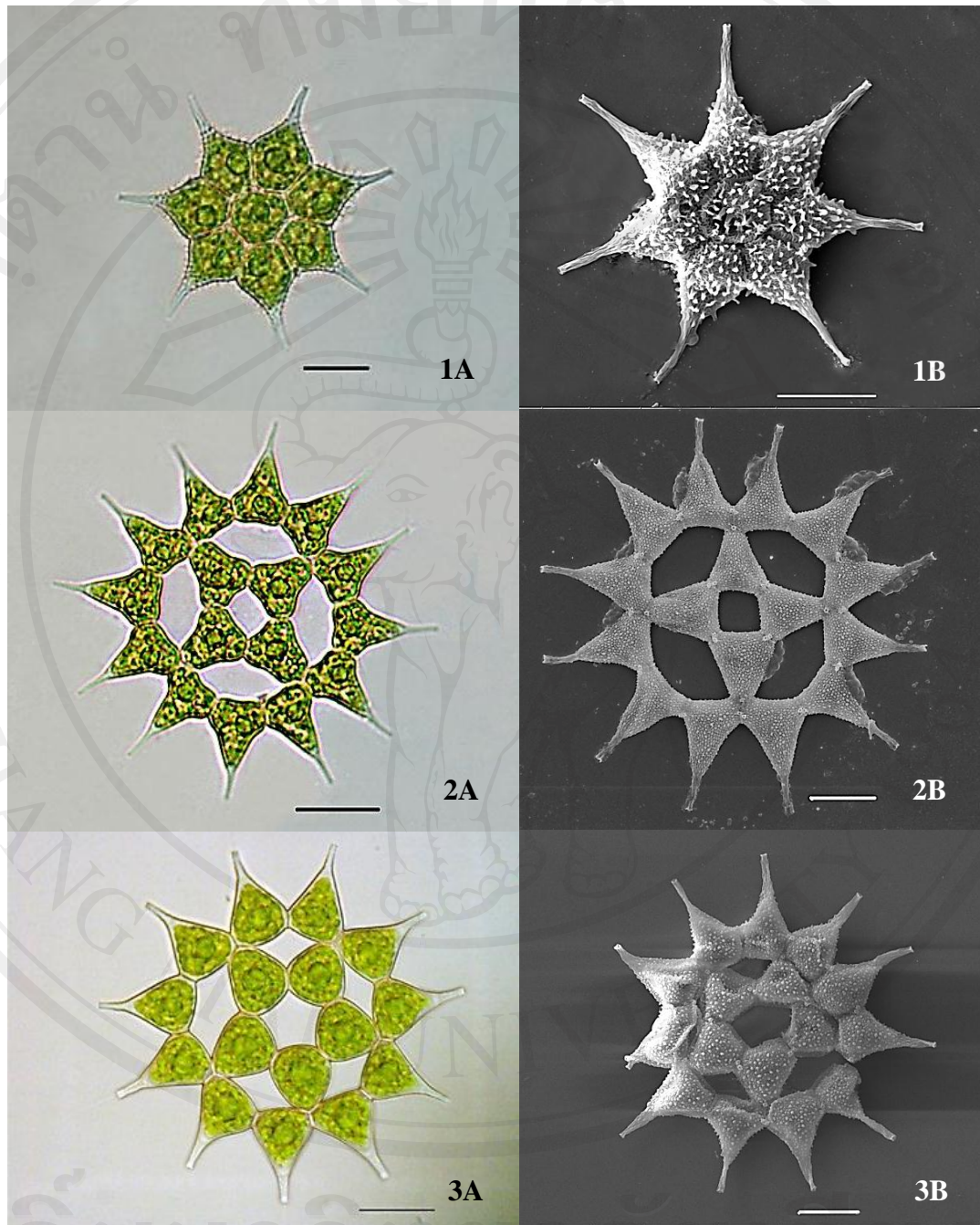


scale bar 10 μm

Figure 7 1A-3A; Light micrographs and 1B-3B; scanning electron micrographs of *Pediastrum* spp.

1A, 1B *P. duplex* var. *asperum* A. Braun, 2A, 2B *P. duplex* var. *duplex* Meyen,

3A, 3B *P. duplex* var. *gracillimum* West & G.S. West

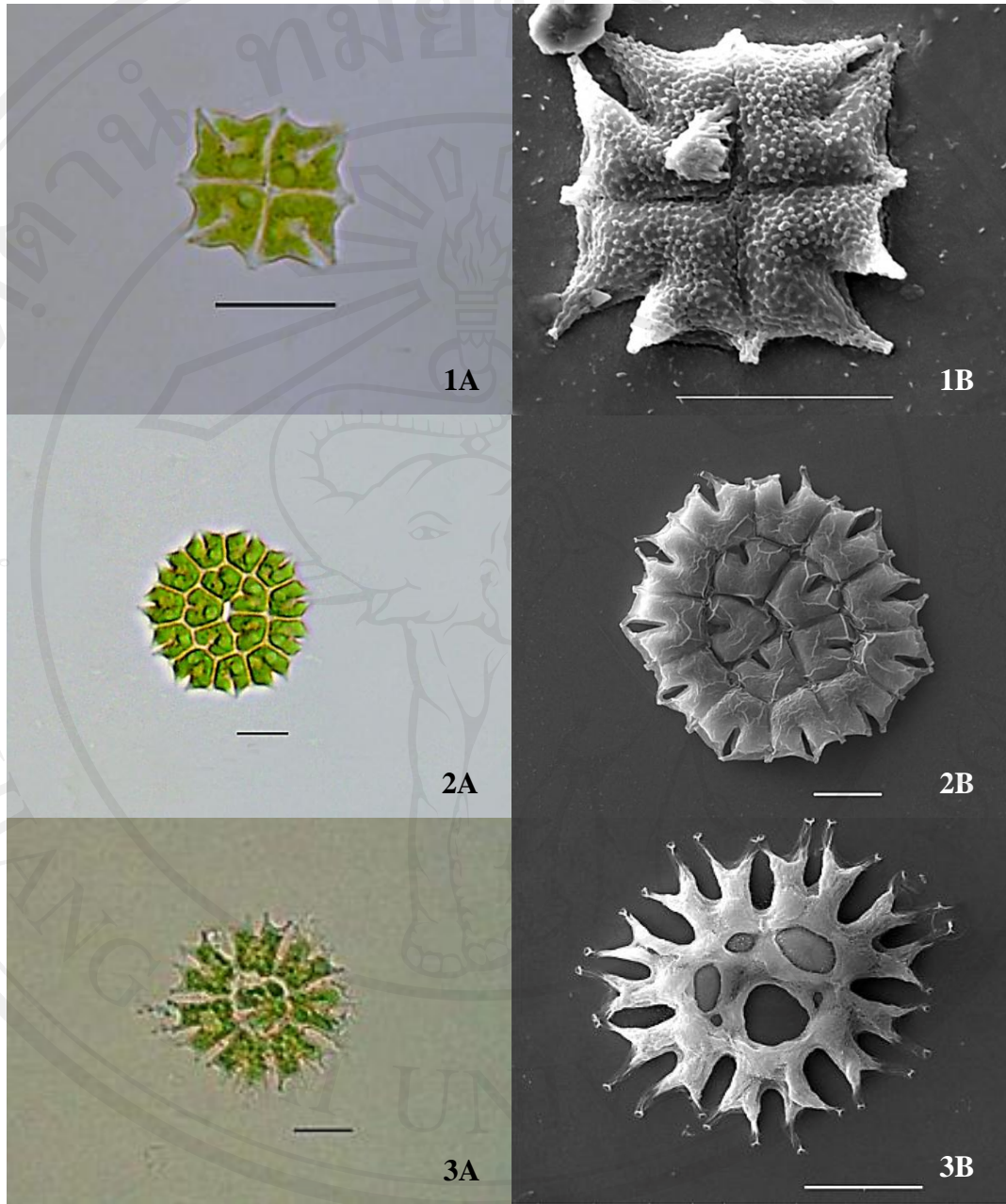


scale bar 10 μm

Figure 8 1A-3A; Light micrographs and 1B-3B; scanning electron micrographs of *Pediastrum* spp.

1A, 1B *P. simplex* var. *echinulatum* Wittrock, 2A, 2B *P. simplex* var. *simplex*

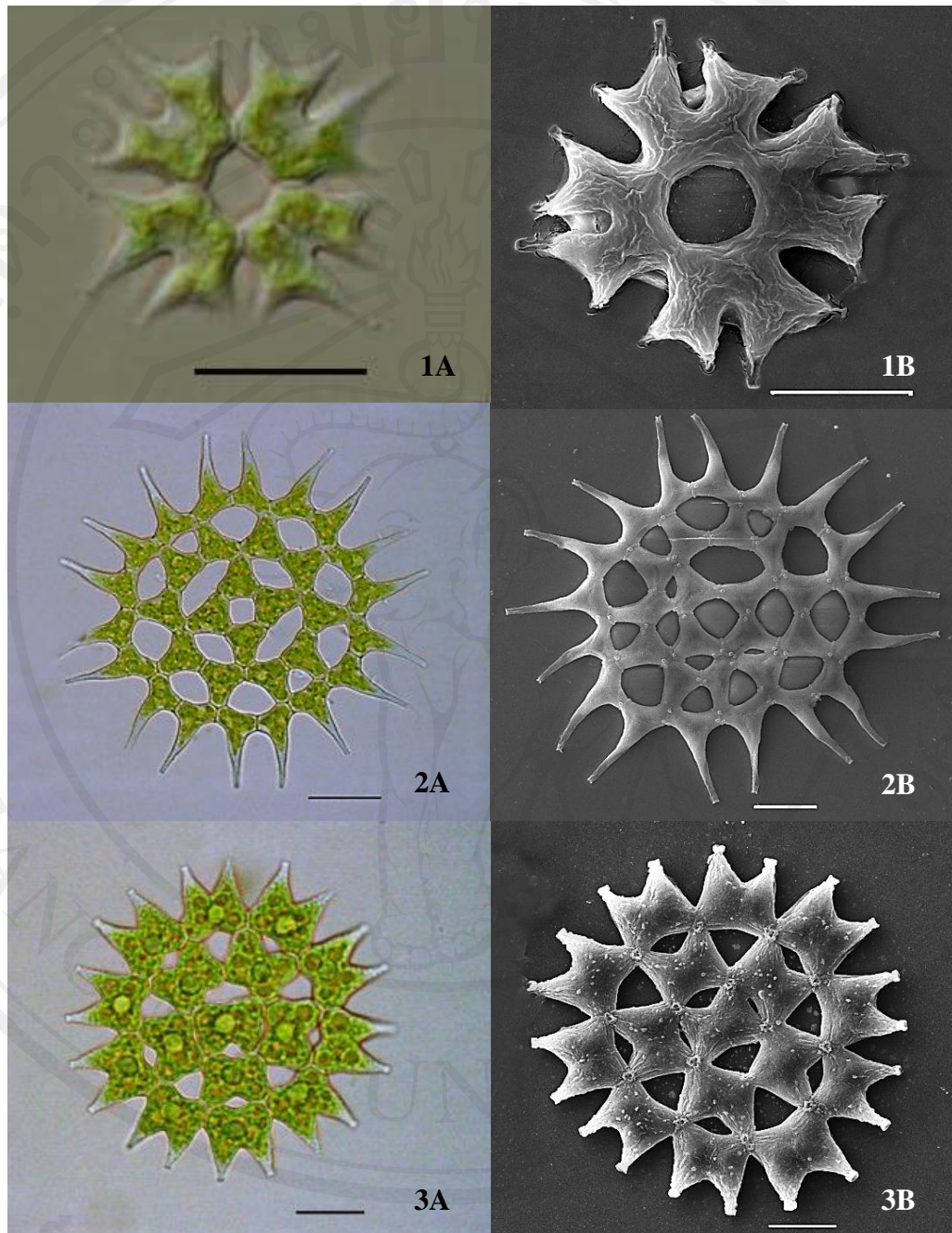
Meyen, 3A, 3B *P. simplex* var. *sturmii* (Reinsch) Wolle



scale bar 10 μm

Figure 9 1A-3A; Light micrographs and 1B-3B; scanning electron micrographs of *Pediastrum* spp.

1A, 1B *P. tetras* var. *tetraodon* (Corda) Hansgirg, 2A, 2B *P. tetras* var. *excisum* Rabenhorst, 3A, 3B *P. longicornutum* Gutwinski



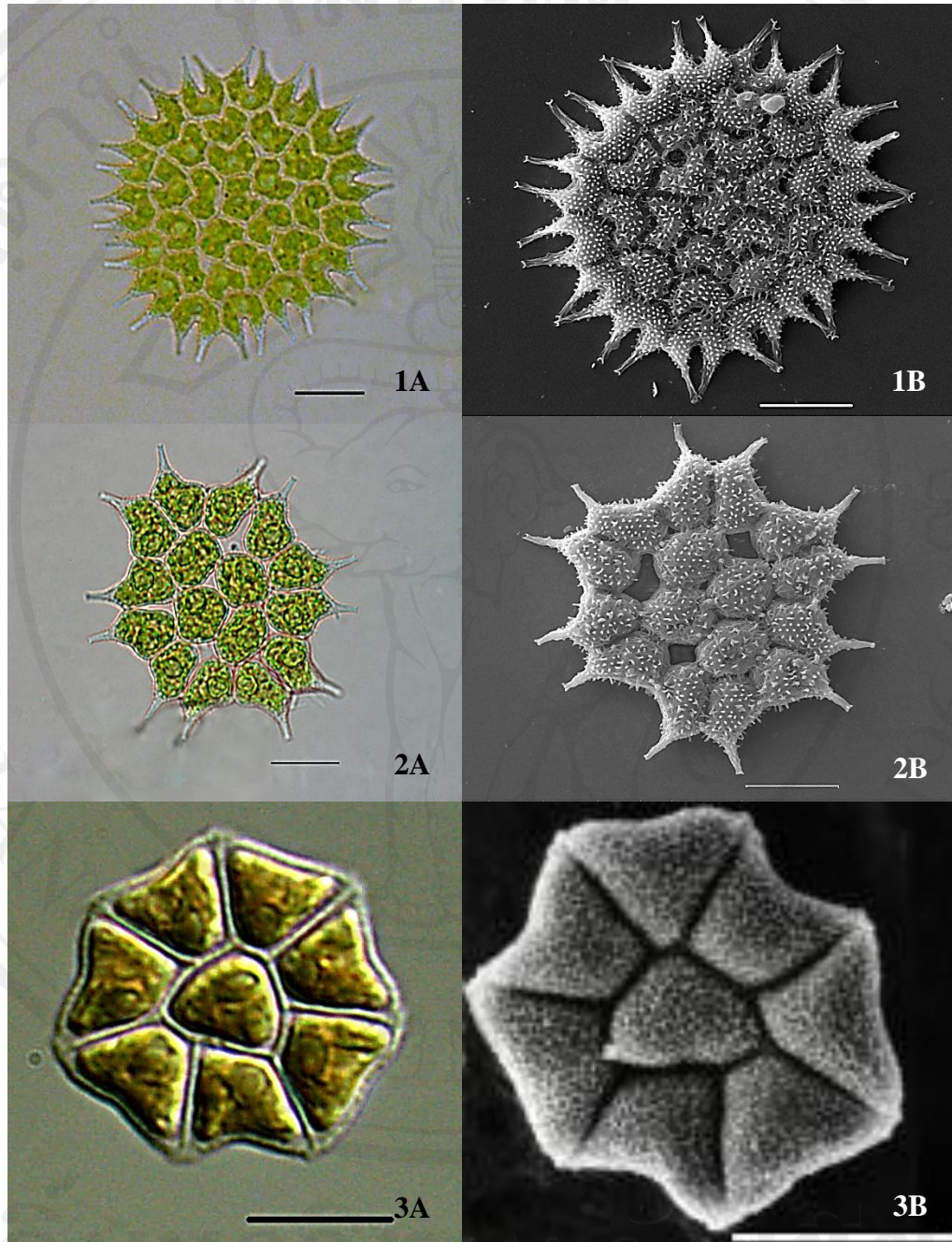
scale bar 10 μ m

Figure 10 1A-3A; Light micrographs and 1B-3B; scanning electron micrographs of

Pediatrum spp.

1A, 1B *P. biradiatum* var. *glabrum* (Raciborski) Parra, 2A, 2B *P. biwae*

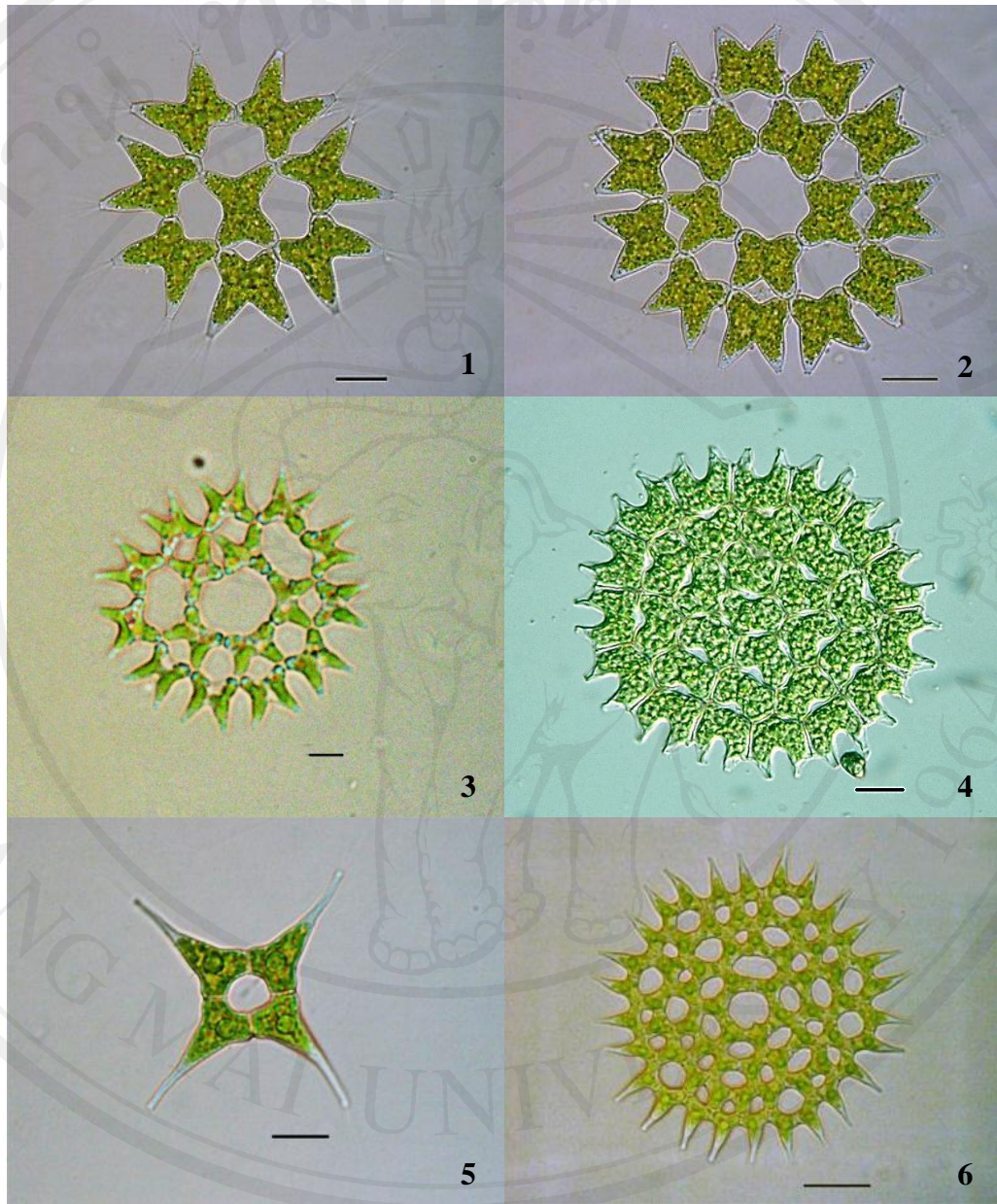
Negoro, 3A, 3B *P. subgranulosum* Raciborski



scale bar 10 μ m

Figure 11 1A-3A; Light micrographs and 1B-3B; scanning electron micrographs of rare species of *Pediastrum* spp.

1A, 1B *Pediastrum alternans* Nygaard, 2A, 2B *P. argentinense* Bourrelly & Tell, 3A, 3B *P. privum* (Printz) E.Hegewald



scale bar 10 μ m

Figure 12 Light micrographs of *Pediastrum* spp. in some freshwater resources of Thailand.

1, 2 *P. duplex* var. *rugulosum* Raciborski, 3. *P. duplex* var. *genuinum* (A.Braun) Lagerheim, 4. *P. angulosum* Ehrenberg ex Meneghini 5. *P. simplex* var. *clathratum* Schröter 6. *P. simplex* var. *duodenarium* (J.W.Bailey) Rabenhorst

Description of new recorded *Pediastrum* species

Pediastrum alternans Nygaard

Coenobium is circular in outline without perforations or with very small, irregular perforations on the outer side of the inner cell (deep incisions of the outer cell). Coenobia are composed of 8-32 cells. Cells are irregularly polygonal within the coenobium. Marginal cells have U-like incision on the outer side. Cell wall ultrastructure is fine wavy or net-like sculpture. Diameter of coenobium is 70-130 μm , cells 12-22 μm wide, 15-28 μm long [Figure 13 (1)].

Distribution: Nakhon Phanom²

Pediastrum angulosum Ehrenberg ex Meneghini

Coenobium is circular, oval or irregular in outline without perforations or small perforations and composed of 16-64 cells. Cells are rectangular or polygonal in outline, joined together at their sides. Marginal cells with two short processes which are conical lobes, situated in the plane of coenobium, processi almost lacking or indistinct, short, terminating continually from the lobes. Between lobes is deep but wide U-like incision or O-like. Lobes are never longer than half of the cell. Cell wall is distinct irregularly net-like sculpture. Coenobium is 70-320 μm , marginal cells are 7-36 μm wide, 8-38 μm long [Figure 13 (2)].

Distribution: Nakhon Si Thammarat² and Songkhla¹

Pediastrum angulosum var. *coronatum* (Raciborski) J.Komárek & V.Jankovská

Coenobium is circular in outline with regularly disposed perforations which appear on the outer sides of inner cells (resulting from deep incisions) usually regular and

circular in outline. Lobes are deep and wide O-like incision. Cell wall is irregularly distinct net-like sculpture. Coenobium is 70-220 μm , marginal cells are 8-26 μm wide, 10-24 μm long [Figure 13 (3)].

Distribution: Khon Kaen² and Si Sa Ket¹

***Pediastrum asymmetricum* Hegewald**

Coenobium is circular in outline with large perforations in young stage and smaller in old stage and composed of 8 or 16 cells. Marginal cells are elongated and paired, creating opening between cells. Eight-celled coenobium has one inner cell and 7 marginal cells, so one marginal cell is not paired but all cells keep their asymmetric form.

Cell wall ultrastructure is densely regularly granular. Marginal cells are 5-11 μm wide, 15-20 μm long. Cells 4-8 μm wide, 8-14 μm long [Figure 13 (4)].

Distribution: Phetchabun¹

***Pediastrum biradiatum* var. *grabrum* Raciborski**

Coenobium is circular in outline with perforations which are usually smaller than the cell diameter. They are composed of 8-32 cells, inner cells are X- shaped, marginal cells with concave sides. The middle is divided into two secondary conical lobes. Diameter of coenobium is 50-82 μm , marginal cells are 8-24 μm wide, 11-30 μm long. Inner cells are 8-21 μm wide, 10-26 μm long [Figure 13 (5)].

Distribution: Chiang Mai³, Phra Nakhon Si Ayutthaya¹, Sing Buri¹, Loei¹, Phatthalung¹ and Songkhla¹

***Pediastrum biwae* Negoro**

Coenobium is circular in outline with perforations. The diameter of holes is larger than the diameter of the cell. Lobes of marginal cells are narrow and the two neighbouring cells always arcuate one to another. Cell wall ultrastructure is smooth or slightly punctuate. Diameter of coenobium is 60-130 μm , cells 7-20 μm wide, 10-35 μm long [Figure 13 (6)].

Distribution: Chiang Mai³, Nakhon Sawan¹, Nakhon Sawan², Uthai Thani¹, Kanchanaburi¹, Kanchanaburi², Phetchaburi¹, Roi Et², Kalasin¹, Nakhon Ratchasima² and Rayong¹

***Pediastrum boryanum* var. *caribeanum* A. Comas**

Coenobium is usually irregular in outline without is circular in outline with perforations or with very few small and irregularly disposed holes and composed of 16-32 cells. Marginal cells have V- shaped incision and deep. Lobes are continually elongated in long process (lobes have process up to 2 times longer than the cell body). Cell wall ultrastructure is finely granulated; granulation visible particularly at the ends of lobes and on process. Diameter of coenobium is 8.5-12.8 μm , process is 6.4-8.5 μm long [Figure 13 (7)].

Distribution: Suphan Buri¹ and Rayong¹

***Pediastrum boryanum* var. *forcipatum* (Corda) Chodat**

Coenobium is circular or slightly irregular in outline, often with irregular arrangement of inner cells. Lobes are very small and conical, process narrow, long

hyaline, incision is shallow V to U shaped and wide in old coenobium. Diameter of coenobium is 80-190 μm , cells 12-23 μm wide, 13-27 μm long [Figure 13 (8)].

Distribution: Chiang Mai³, Sukhothai¹ and Phichit¹

***Pediastrum boryanum var. longicone* Reinsch**

Coenobium is circular in outline with perforations or with very few small perforations and composed of 4-64 cells. Marginal cells have V- shaped incision and deep. Process is long or sometimes slightly curved at the end and sometimes slightly widened. Cell wall ultrastructure is scarcely and distinctly granular. Diameter of coenobium is 80-248 μm , cells 2-10 μm wide, 4-15 μm long [Figure 13 (9)].

Distribution: Nakhon Phanom², Nakhon Ratchasima² and Rayong¹

***Pediastrum boryanum var. perforatum* (Raciborski) Nitardy**

Coenobium is circular in outline without is circular in outline with perforations or small perforations and composed of 4-32 cells. Incisions are wide and V- shaped. Process is long. Cell wall ultrastructure is very distinctly granular. Diameter of coenobium is 70-120 μm , cells 8-21 μm wide, 8-26 μm long [Figure 13 (10)].

Distribution: Chiang Mai³ and Nakhon Phanom²

***Pediastrum boryanum var. pseudoglabrum* Parra**

Coenobium is circular in outline without perforations and composed of 4-32 cells. Marginal cells have V- shaped incision. Cell wall ultrastructure is very finely granular. Diameter of coenobium is 20-96 μm , wide, 8-14 μm long [Figure 13 (11)].

Distribution: Chiang Mai³ and Nakhon Ratchasima²

***Pediastrum duplex* var. *asperum* A. Braun**

Coenobium is circular in outline and composed of 16-64 cells. Perforation in coenobium is always smaller than the cell diameter. Cell wall ultrastructure is irregularly net-like sculpture. Diameter of coenobium is 90 μm , cells 8-18 μm wide, 8-19 μm long [Figure 13 (12)].

Distribution: Phayao², Uttaradit¹, Phichit¹, Ang Thong¹, Suphan Buri¹, Uthai Thani¹, Surin¹, Chachoengsao¹, Rayong¹, Rayong², Kanchanaburi¹, Nakhon Si Thammarat¹ and Phatthalung¹

***Pediastrum duplex* var. *coronatum* Raciborski**

Coenobium is circular in the outline, with a small lens – shaped perforations in the front and another at the back. Marginal cells are usually longer than wide and in lateral contact along one-third of the length. Processes of marginal cells ending are short spines. Coenobium is composed of 16-32-64 cells. Cell wall ultrastructure varies from net-like to warty. Diameter of coenobium is 120-214 μm , marginal cells 21-25 μm wide, 25-25 μm long [Figure 13 (13)].

Distribution: Chiang Mai³, Rayong¹ and Phatthalung¹

***Pediastrum duplex* var. *genuinum* (A.Braun) Lagerheim**

Coenobium is circular in the outline and composed of 4-32 cells with fairly large intercellular spaces. Marginal cells with stout processes which are straight or slightly curved. Cell wall ultrastructure is smooth or punctate. Diameter of coenobium is 45-65 μm , cells 5-7 μm wide, 6-8 μm long. [Figure 13 (14)].

Distribution: Uttaradit¹ and Chanthaburi¹

***Pediastrum integrum* var. *perforatum* Raciborski**

Coenobium is circular in outline, with a small perforations and composed of 8- 2 cells. Peripheral cells of similar shape joined to each other at the base but free on the outside with two short truncate processes from the outer face one from each side. Diameter of coenobium is 70-110 μm , cells 12-17 μm wide, 14-18 μm long [Figure 13 (15)].

Distribution: Chanthaburi¹ and Surat Thani¹

***Pediastrum kawraiskyi* Schmidle**

Coenobium is circular in the outline, rarely irregular, always without perforations between cells. Coenobium is composed of 4-32 cells which are concentrically arranged and completely joined at their sides. Cells are irregularly polygonal in the coenobium center with straight sides. Marginal cell is elongated into one wide, massive lobe which divides approximately in its half-length into two conical secondary lobe. Cell wall ultrastructure is irregularly and sometime indistinctly granular. Diameter of coenobium is 50-100 μm , cells 4.6-15.2 μm wide, 6.6-17.9 μm long [Figure 13 (16)].

Distribution: Chiang Rai¹ and Songkhla¹

***Pediastrum muticum* Kützing**

Coenobium is circular in outline without perforations or small perforations and composed of 8-64 cells. Marginal cells are inverted heart-shaped, with or without two short processes on the free side. Cell wall ultrastructure is smooth or granular. Diameter of coenobium is 50-120 μm , cells 19-21 μm wide, 21-25 μm long [Figure 13(17)].

Distribution: Phrae¹ and Nakhon Si Thammarat²

***Pediastrum primum* (Printz) E.Hegewald**

Coenobium is circular or rounded, square shaped in outline without perforations with completely joined cell sides, and composed of 4-8 cells. There is a very fine, diffiuent, colorless mucilaginous envelope around the coenobium. Cells are 5-7gonal with straight side. Chloroplast does not always cover the whole cell wall (as in other species) pyrenoid is sometime indistinct. Marginal cells are 3-5 gonal, on the outer side with very shallow concavity (indistinct, very wide and very shallow V-like depression). On both outer “corners” of marginal cell, near the connecting walls with the neighbouring cells. There is small, wart- like thickening. Cell wall ultrastructure is very fine, irregularly, net-like (wavy) sculpture. Diameter of a coenobium is 5-25 μm , cells 3.5-7 μm wide, 5-12 μm long. [Figure 13 (18)].

Distribution: Chiang Mai³

***Pediastrum simplex* var. *pseudoglabrum* Parra**

Coenobium is circular in the outline with perforations. Diameter of the perforations is usually larger than the cell diameter. Cell wall ultrastructure is smooth. Diameter of coenobium is 80 μm , marginal cells are 10-17 μm wide, 11-20 μm long [Figure 13 (19)].

Distribution: Chiang Mai³, Sukhothai¹, Nakhon Sawan², Pathum Thani¹, Uthai Thani¹, Khon Kaen¹, Sa Kaeo¹, Surat Thani² and Nakhon Si Thammarat³

***Pediastrum subgranulatum* Raciborski**

Coenobium is circular in outline and composed of 8-16-64 cells with regularly disposed perforations (perforations are always of smaller diameter than the cell diameter).

Marginal cells have two long prominent radial conical lobes usually longer than the cell body. Cell wall ultrastructure are varies from irregularly, densely and distinctly granular. Diameter of coenobium is 120 μm , marginal cells 5.5-28.5 μm wide, 5-25 μm long, inner cells 4-20 μm wide, 5-25 μm long [Figure 13 (20)].

Distribution: Chiang Mai³, Ang Thong¹, Loei¹, Rayong¹, TAK¹ and Songkhla¹

***Pediastrum tetras var. aciculatum* Fritsch**

Coenobium is circular or rectangular in outline, lack of perforations and composed of 4-32 cells. Marginal cells have narrow incisions and are trapezoidal in shape. Marginal cell are divided into two lobes and slightly concave, each lobe truncated.

Cell wall ultrastructure varies from irregularly net-like to warty. Diameter of coenobium is 80 μm , cells 6-18 μm wide, 8-19 μm long [Figure 13 (21)].

Distribution: Chiang Mai³, Loei¹ and Chon Buri¹

***Pediastrum tetras var. excisum* Rabenhorst**

Coenobium is circular or rectangular in outline, composed of 4-32 cells and lack of perforations. Marginal cells have narrow incisions and are trapezoidal in shape. Marginal cell are divided into two lobes and slightly concave, each lobe truncated. Cell wall ultrastructure is very fine. Diameter of coenobium is 8-80 μm , cells 5-16 μm wide, 6-19 μm long [Figure 13 (22)].

Distribution: Chiang Mai³, Suphan Buri¹, Uthai Thani¹, Uthai Thani², Ubon Ratchathani¹, Nakhon Si Thammarat¹, Phatthalung¹ and Songkhla¹

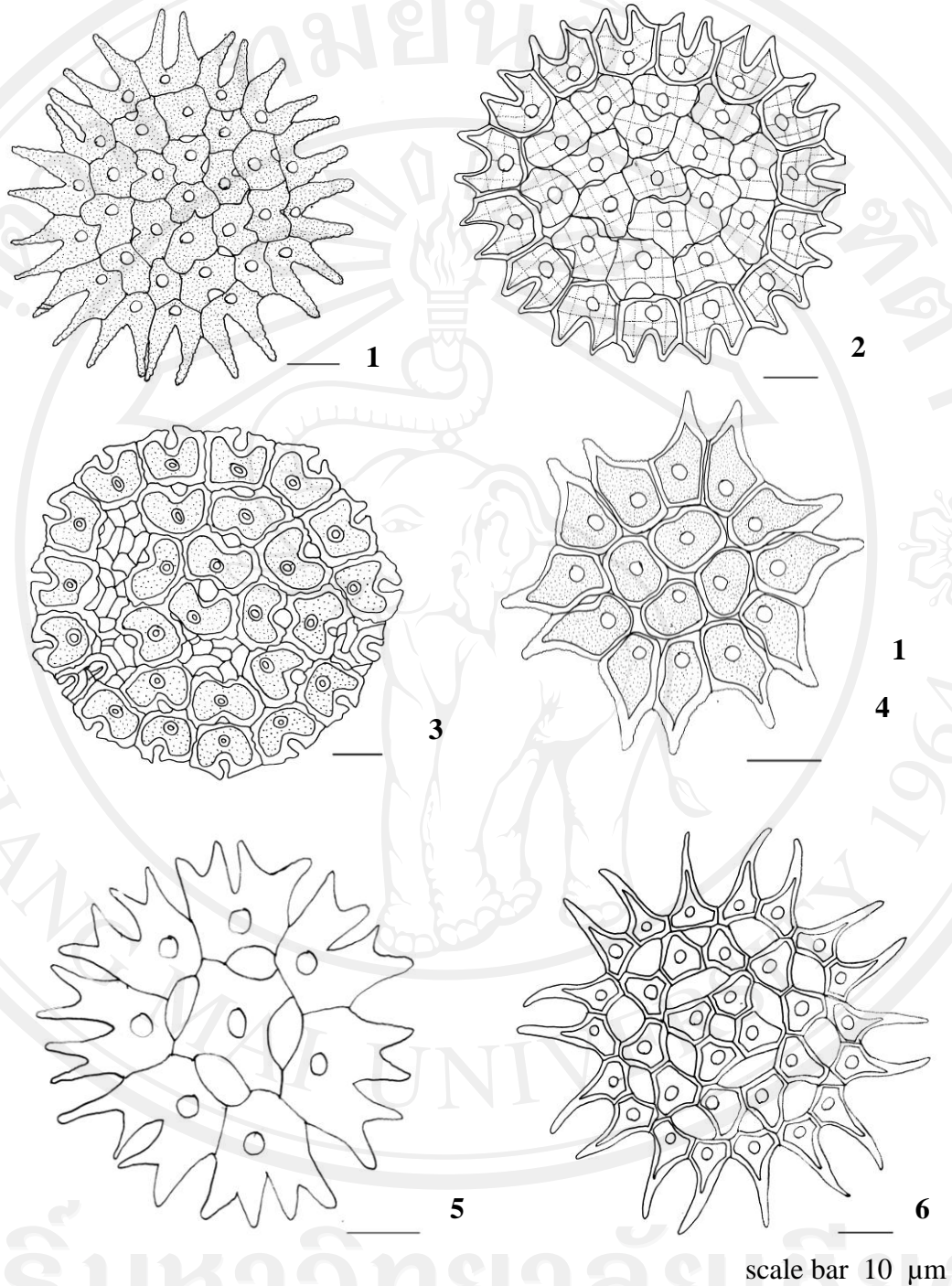


Figure 13 Illustration of new record of *Pediatrum* spp. of Thailand

1. *Pediatrum alternans* Nygaard, 2. *P. angulosum* Ehrenberg ex Meneghini,
3. *P. angulosum* var. *coronatum* (Raciborski) J.Komárek & V.Jankovská,
4. *P. asymmetricum* T.Yamagishi & E.Hegewald, 5. *P. biradiatum* var. *glabrum* (Raciborski) Parra, 6. *P. biwae* Negoro

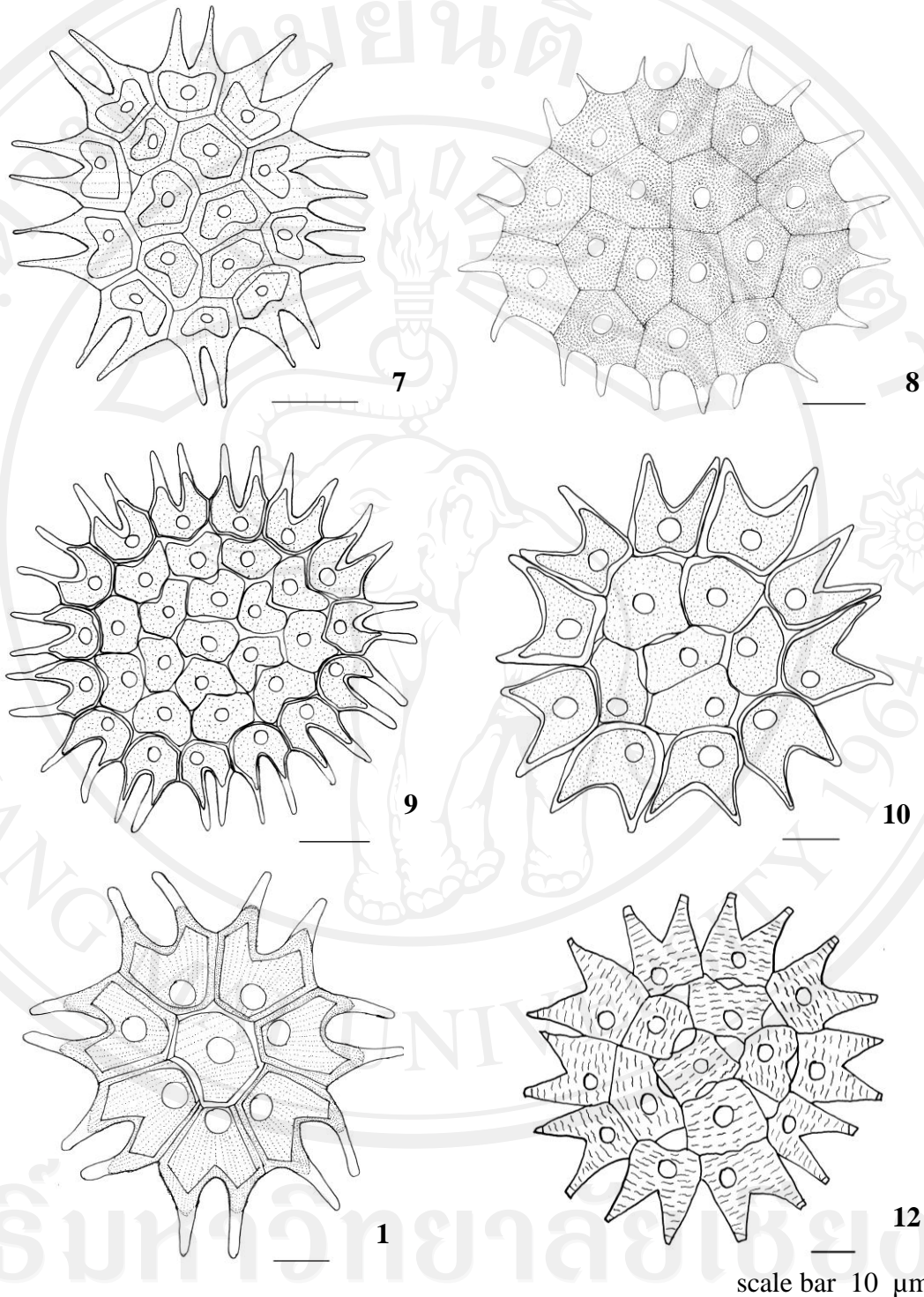


Figure 13 Continued. 7. *P. boryanum* var. *caribeanum* A.Comas, 8. *P. boryanum* var. *forcipatum* (Corda) Chodat, 9. *P. boryanum* var. *longicorne* Reinsch 10. *P. boryanum* var. *perforatum* (Raciborski) Nitardy, 11. *P. boryanum* var. *pseudoglabrum* Parra Barrientos, 12. *P. duplex* var. *asperum* A.Braun

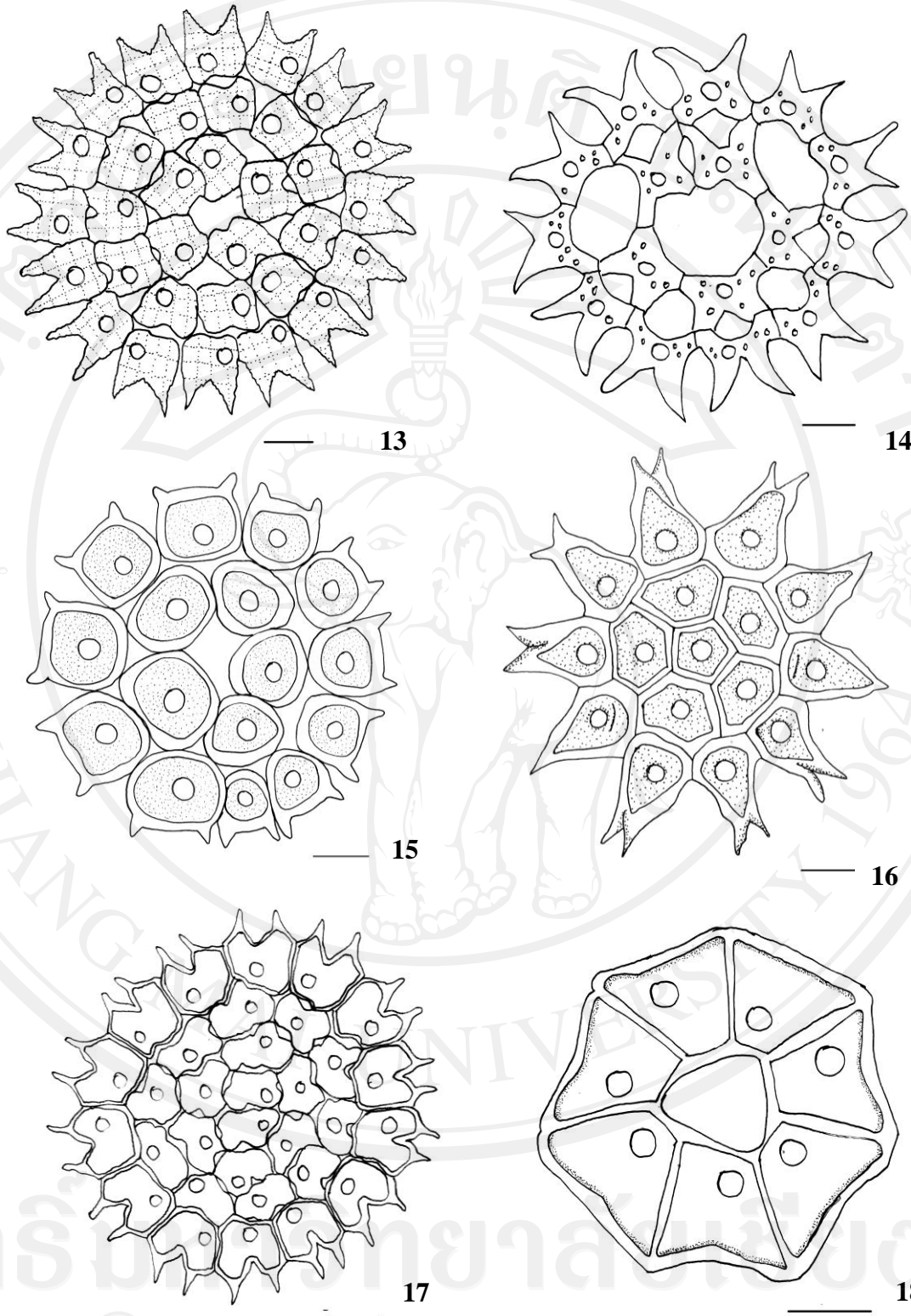
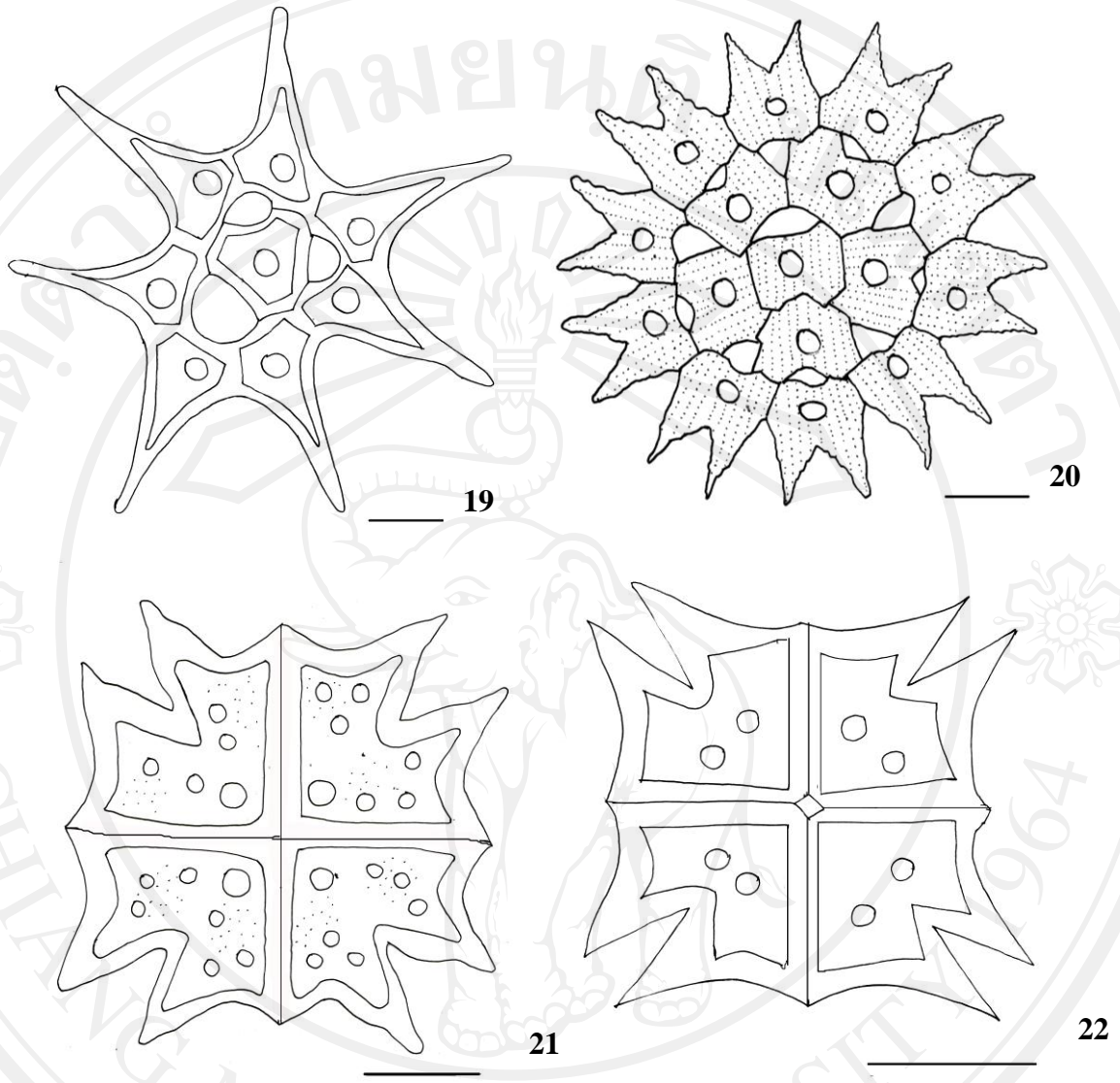
scale bar 10 μm

Figure 13 Continued. 13. *P. duplex* var. *coronatum* Raciborski, 14. *P. duplex* var. *genuinum* (A. Braun) Lagerheim, 15. *P. integrum* var. *perforatum* Raciborski, 16. *P. kawraiskyi* Schmidle, 17. *P. muticum* Kützing, 18. *P. privum* (Printz) E. Hegewald



scale bar 10 μ m

Figure 13 Continued. 19. *P. simplex* var. *pseudoglabrum* Parra Barrientos, 20. *P. subgranulosum* Raciborski, 21. *P. tetras* var. *apiculatum* Playfair and 22. *P. tetras* var. *excisum* Rabenhorst

4.3 *Pediastrum* spp. distribution and physico-chemical parameters

4.3.1 Air and water temperature

Air and water temperature of freshwater resources at 68 sites in Thailand depended on latitude, altitude, time of day and season. The ranges of air and water temperature were 17-37 °C and 20.3-34.5 °C respectively. The highest air temperature was found at SRT3 and the lowest at LOE1. Water temperature was highest at SRT3 and lowest at NPN2 (Figures 14 and 15).

4.3.2 Turbidity

The type and concentration of suspended matter control the turbidity and transparency of water. Suspended matter consists of silt, clay, fine particles of organic and inorganic matter, soluble organic compounds and plankton. The ranges of turbidity at each sampling site varied from 7-323 NTU with the highest value at RYN2 and the lowest at KCN2 (Figure 16).

4.3.3 pH

The pH value is a measure of the acid balance of solution and defined as the negative of the logarithm to the base 10 of the hydrogen ion concentration. The pH scale runs from 0-14 (i.e. very acidic to very alkaline), with pH 7.0 representing a neutral condition. pH is principally controlled by the balance between the carbon dioxide, carbonate and bicarbonate ion. The ranges of pH at each sampling site varied from 5.12-10.29 with the highest value at CBR1 and the lowest at SRT3 (Figure 17).

4.3.4 Alkalinity

The alkalinity of water is controlled by the sum of titratable bases. It is mostly taken as an indication of the concentration of carbonate (CO_3^{2-}), bicarbonate (HCO_3^-) and hydroxide (OH^-). The ranges of alkalinity at each sampling site varied from 9.3-290.7 mg/L as CaCO_3 with the highest value at NKS2 and the lowest at NPN2 (Figure 18).

4.3.5 Conductivity

Conductivity is a measure of the ability of water to conduct an electric current. It is sensitive to variation in dissolved solids, mostly mineral salts. The ranges of conductivity at each sampling site varied from 30.8- 1863.5 $\mu\text{S}/\text{cm}$ with the highest value at RYN1 and the lowest at NST2 (Figure 19).

4.3.5 Dissolved oxygen (DO)

Oxygen is one of the most important factors for water quality and the associated aquatic life. The oxygen content of natural waters varies with temperature, salinity, turbulence, the photosynthetic activity of algae and plant and atmospheric pressure. The solubility of oxygen decrease as temperature and salinity increase. The ranges of DO at each sampling site varied from 3.0- 22.0 mg/L with the highest value at NRS1 and the lowest at CCS1 (Figure 20).

4.3.6 Biochemical oxygen demand (BOD)

Biochemical oxygen demand is an approximate measure of the amount of biochemically degradable organic matter present in water in a water sample. It is defined

by the amount of oxygen required for the aerobic micro-organisms in the sample to oxidize the organic matter to a stable inorganic form. The ranges of BOD at each sampling site varied from 0.3- 18.7 mg/L with the highest value at SKT1 and the lowest at CCS1 (Figure 21).

4.3.7 Ammonium nitrogen

Ammonia occurs naturally in water bodies arising from the breakdown of nitrogenous organic and inorganic matter in soil and water, excretion by biota, reduction of the nitrogen gas in water by micro-organism and from gas exchange with the atmosphere. The ranges of ammonium nitrogen at each sampling site varied from (non detect) nd – 5.69 mg/L with the highest value at SKN1 and the lowest at SSK1, RBR1 and STN1 (Figure 22).

4.3.8 Nitrate nitrogen

The nitrate ion (NO_3^-) is the common form of combined nitrogen found in natural water. It may be biochemically reduced to nitrite (NO_2^-) by denitrification processes, usually under anaerobic conditions. The nitrite ion is rapidly oxidized to nitrate. Nitrate is an essential nutrient for aquatic plants and seasonal fluctuations can be caused by plant growth and decay. The ranges of nitrate nitrogen at each sampling site varied from nd– 1.9 mg/L with the highest value at UDT1 and the lowest at PSL1, PTT1, SUR2, SSK1,SKO1 and RBR1 (Figure 23).

4.3.9 Soluble reactive phosphorus

Phosphorus is an essential nutrient for living organisms and exists in water bodies as both dissolved and particulate species. It is generally the limiting nutrient for algal growth and therefore, controls the primary productivity of a water body. High concentrations of phosphates can indicate the presence of pollution and are largely responsible for eutrophic conditions. The ranges of soluble reactive phosphorus at each sampling site varied from 0.00 – 3.00 mg/L with the highest value at SUR1 and the lowest at NPN1, NPN2, MDH2, KLS1, CTB1 and SRT1 (Figure 24).

4.3.10 Chlorophyll *a*

The green pigment chlorophyll (which exists in tree forms: Chlorophyll *a*, *b* and *c*) is present in most photosynthetic organisms and provides an indirect measure of algal biomass and an indication of the trophic status of a water body. The ranges of chlorophyll *a* at each sampling site varied from 2.7 – 637 µg/L with the highest value at SUR1 and the lowest at KLS1 (Figure 25).

4.4 Water quality and trophic status by AARL-PC Score

The trophic status of the water was evaluated from the main parameters, which were: conductivity, DO, BOD, ammonium nitrogen, nitrate nitrogen, soluble reactive phosphorus and chlorophyll *a* by the Applied Algal Research Laboratory Physical and Chemical Score (AARL-PC Score) method of Peerapornpisal *et al.* (2007) which was based on Wetzel (2001); Lorraine and Vollenweider (1981). The trophic status and

AARL-PC Score of the water at each sampling site are shown in Figure 26. The water qualities were generally classified into 5 trophic levels i.e. oligo-mesotrophic, mesotrophic, meso-eutrophic, eutrophic and hypereutrophic (Figure 27). It was demonstrated that 13.2% (9 sampling sites) were oligo-mesotrophic and the water quality was clean-moderate, 36.8% (25 sampling sites) were mesotrophic and the water quality was moderate, 41.2% (28 sampling sites) were meso-eutrophic and the water quality was moderate-polluted, 5.9% (4 sampling sites) were eutrophic and the water quality was polluted, 2.9% (2 sampling sites) were hypereutrophic and the water quality was very polluted.

4.5 Canonical correspondence analysis (CCA) of physico-chemical parameters and *Pediastrum* spp.

The results of the CCA of some physico-chemical parameters and *Pediastrum* spp. with high relative abundance (>1%) are showed in CCA plot (Figure 28). It was found that *P. angulosum* var. *coronatum*, *P. biradiatum*, *P. biradiatum* var. *emarginatum*, *P. biradiatum* var. *glabrum*, *P. biwae*, *P. boryanum* var. *boryanum*, *P. boryanum* var. *longicorne*, *P. boryanum* var. *perforatum*, *P. boryanum* var. *pseudoglabrum*, *P. simplex* var. *simplex*, *P. simplex* var. *echinulatum* and *P. simplex* var. *pseudoglabrum* had a positive correlation with Secchi depth and negative correlation with water temperature, pH, BOD, Turbidity, soluble reactive phosphorus (PO_4^{2-}), and chlorophyll *a* thus the taxa were found in high abundance when the water conditions displayed a high Secchi depth and low water temperature, pH, BOD, Turbidity, soluble reactive phosphorus, and could

be used to monitor the clean-moderate to indicate water quality. The presence of *P. araneosum*, *P. asymmetricum*, *P. boryanum* var. *cornutum*, *P. duplex* var. *duplex* and *P. duplex* var. *gracillimum* had a positive correlation with pH, BOD depth and negative correlation with Secchi thus the taxa were found in high abundance when the water conditions displayed a high pH, BOD and low Secchi depth and could be used to monitor the moderate-polluted to indicate water quality. The presence of *P. boryanum* var. *forcipatum* and *P. duplex* var. *genuinum* had a positive correlation with water temperature, soluble reactive phosphorus and Chlorophyll *a* and negative correlation with Secchi depth thus the taxa were found in high abundance when the water conditions displayed a high water temperature, soluble reactive phosphorus and Chlorophyll *a* and low Secchi depth and could be used to monitor the polluted to indicate water quality. The presence of *P. boryanum* var. *brevicorne*, *P. clathratum*, *P. duplex* var. *clathralum*, *P. duplex* var. *cohaerens*, *P. duplex* var. *rotundatum*, *P. emarginatum* and *P. pertusum* had a positive correlation with air temperature, alkalinity, conductivity and nitrate nitrogen and negative correlation with DO thus the taxa were found in high abundance when the water conditions displayed a high air temperature, alkalinity, conductivity and nitrate nitrogen and low DO and could be used to monitor the moderate-polluted to indicate water quality.

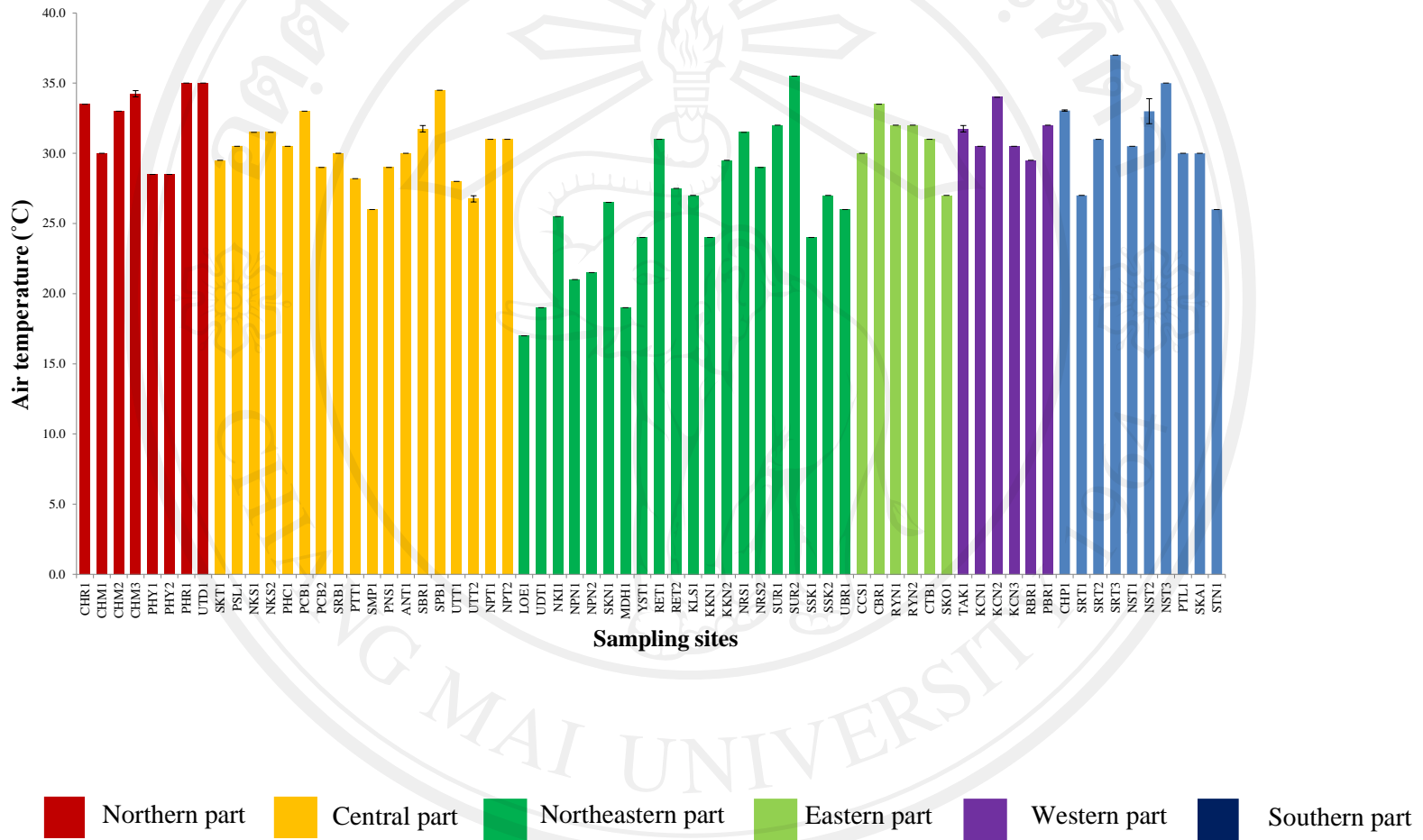


Figure 14 Air temperatures at 68 sampling sites

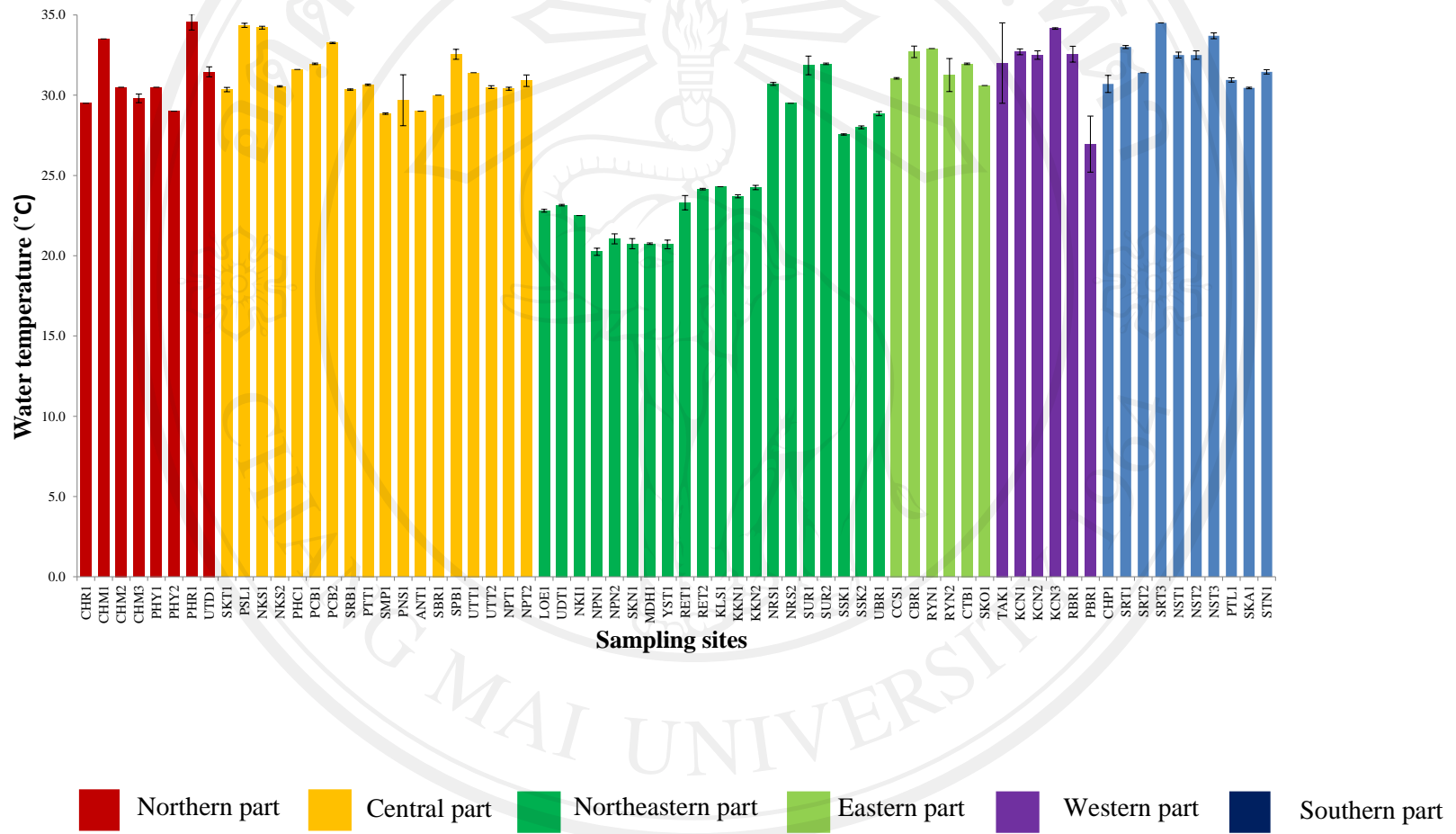
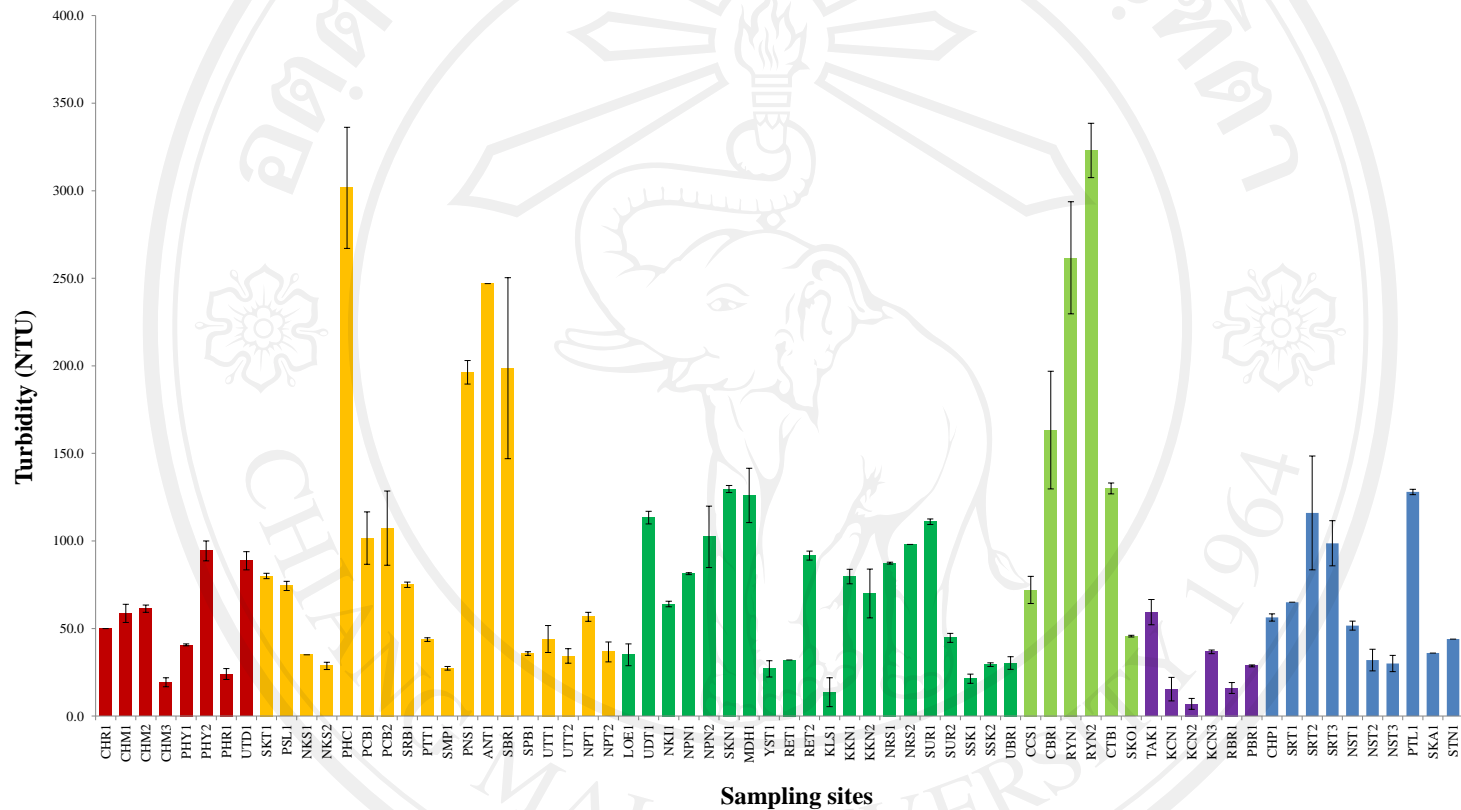


Figure 15 Water temperatures at 68 sampling sites

ลิขสิทธิ์มหาวิทยาลัยเชียงใหม่
 Copyright © by Chiang Mai University
 All rights reserved



■ Northern part
 ■ Central part
 ■ Northeastern part
 ■ Eastern part
 ■ Western part
 ■ Southern part

Figure 16 Turbidity of water at 68 sampling sites

ลิขสิทธิ์มหาวิทยาลัยเชียงใหม่
 Copyright © by Chiang Mai University
 All rights reserved

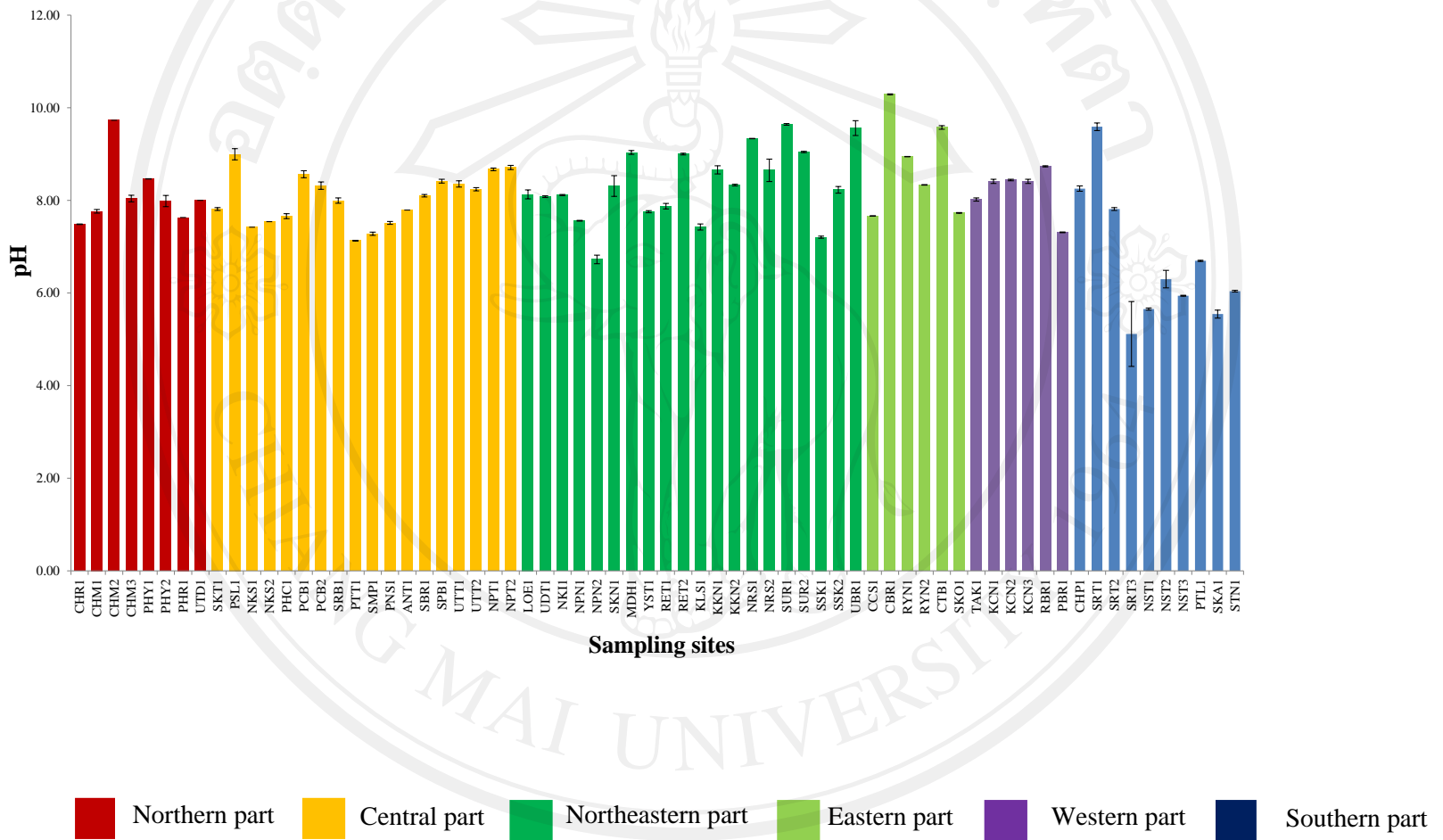
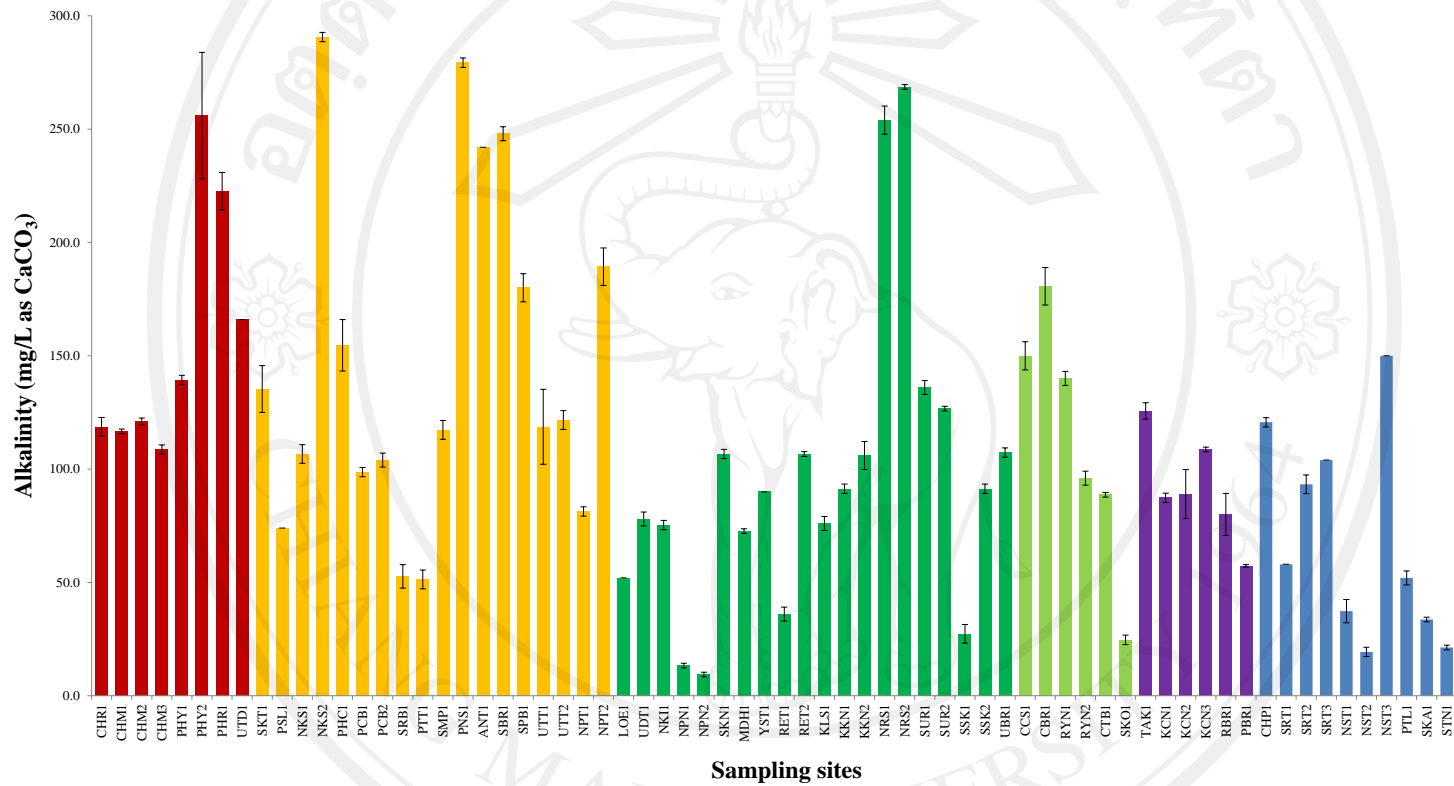


Figure 17 pH of water at 68 sampling sites

ลิขสิทธิ์มหาวิทยาลัยเชียงใหม่
 Copyright © by Chiang Mai University
 All rights reserved



■ Northern part
 ■ Central part
 ■ Northeastern part
 ■ Eastern part
 ■ Western part
 ■ Southern part

Figure 18 Alkalinity of water at 68 sampling sites

ลิขสิทธิ์มหาวิทยาลัยเชียงใหม่
 Copyright © by Chiang Mai University
 All rights reserved

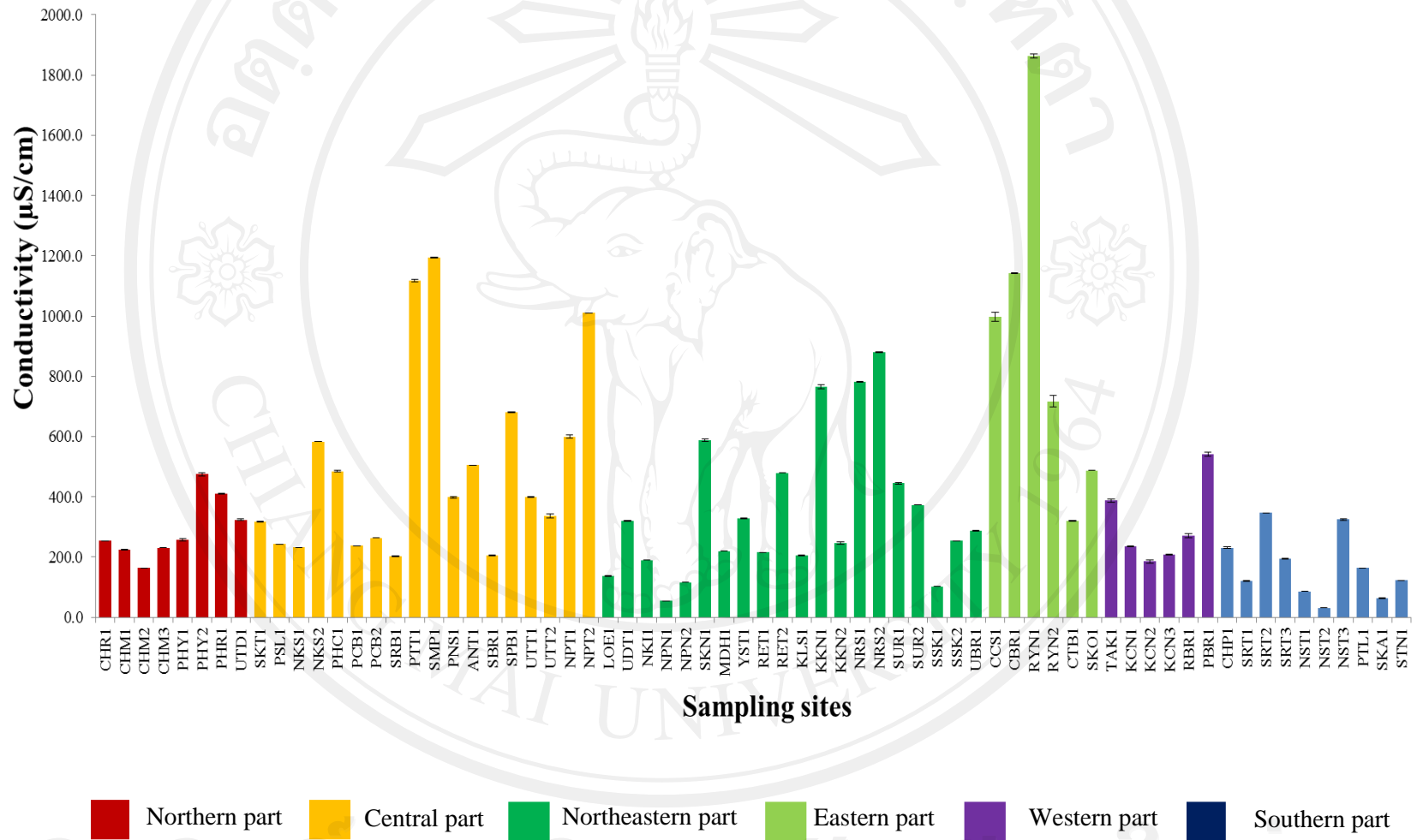


Figure 19 Conductivity of water at 68 sampling sites

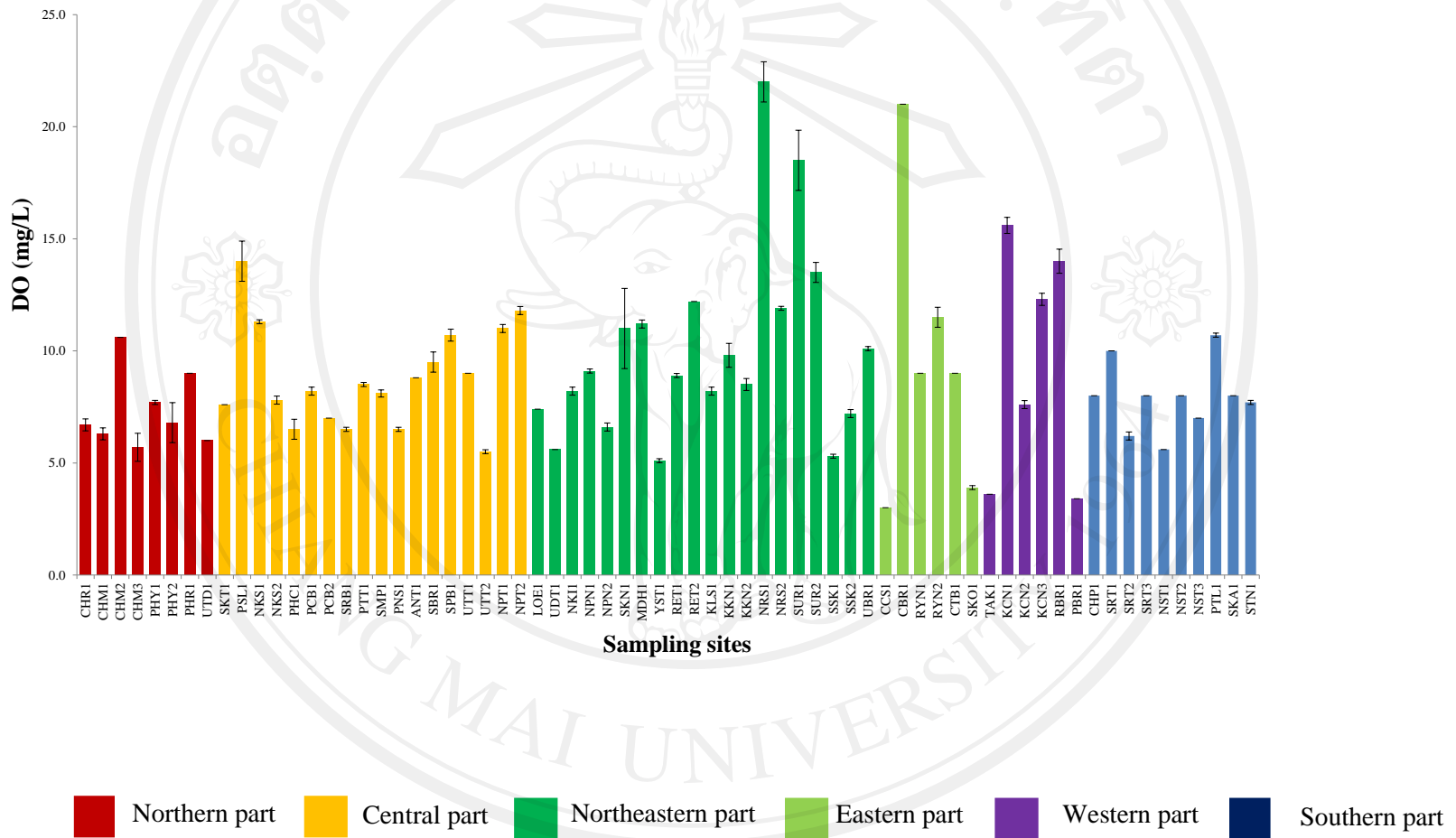


Figure 20 Dissolved oxygen of water at 68 sampling sites

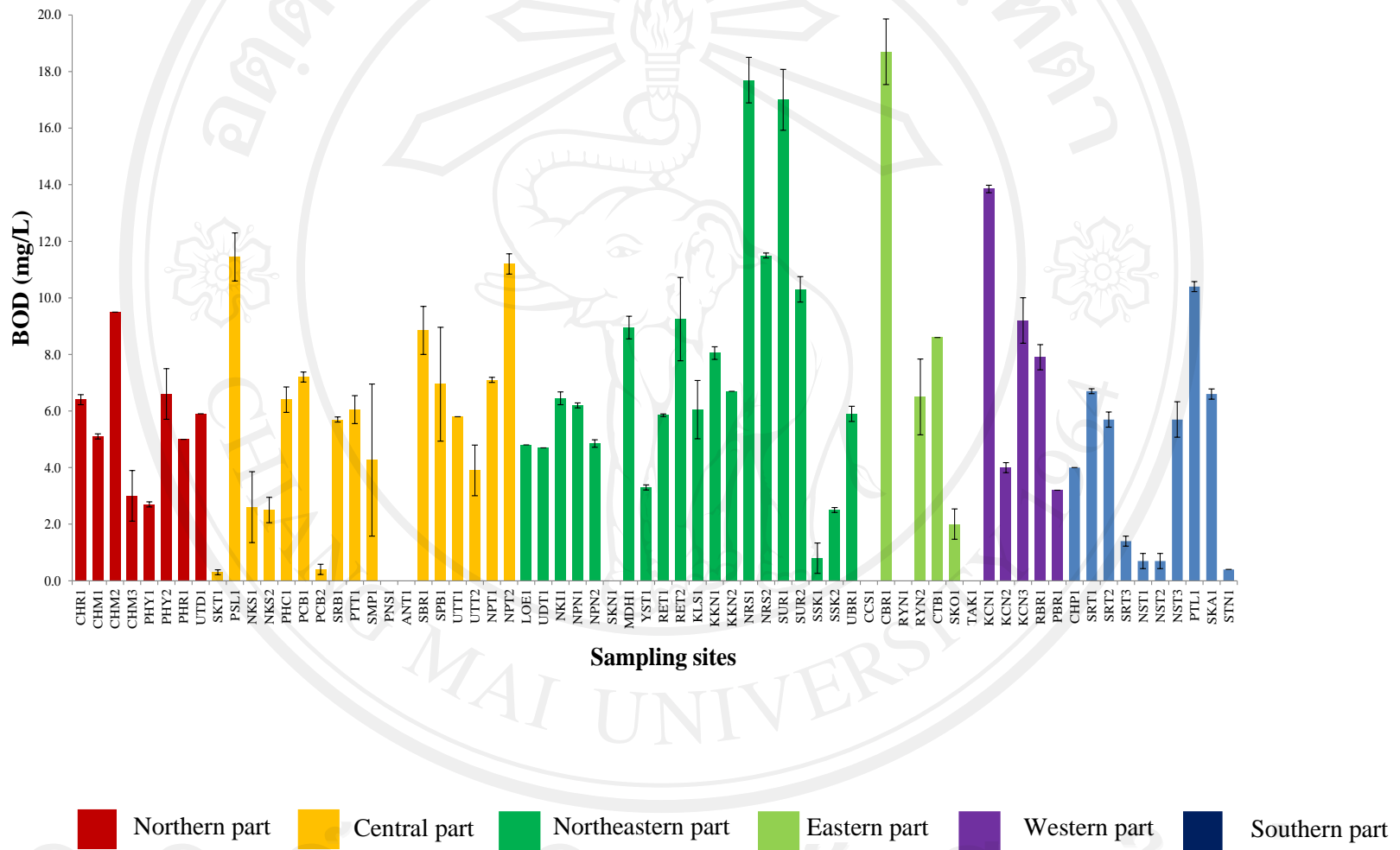
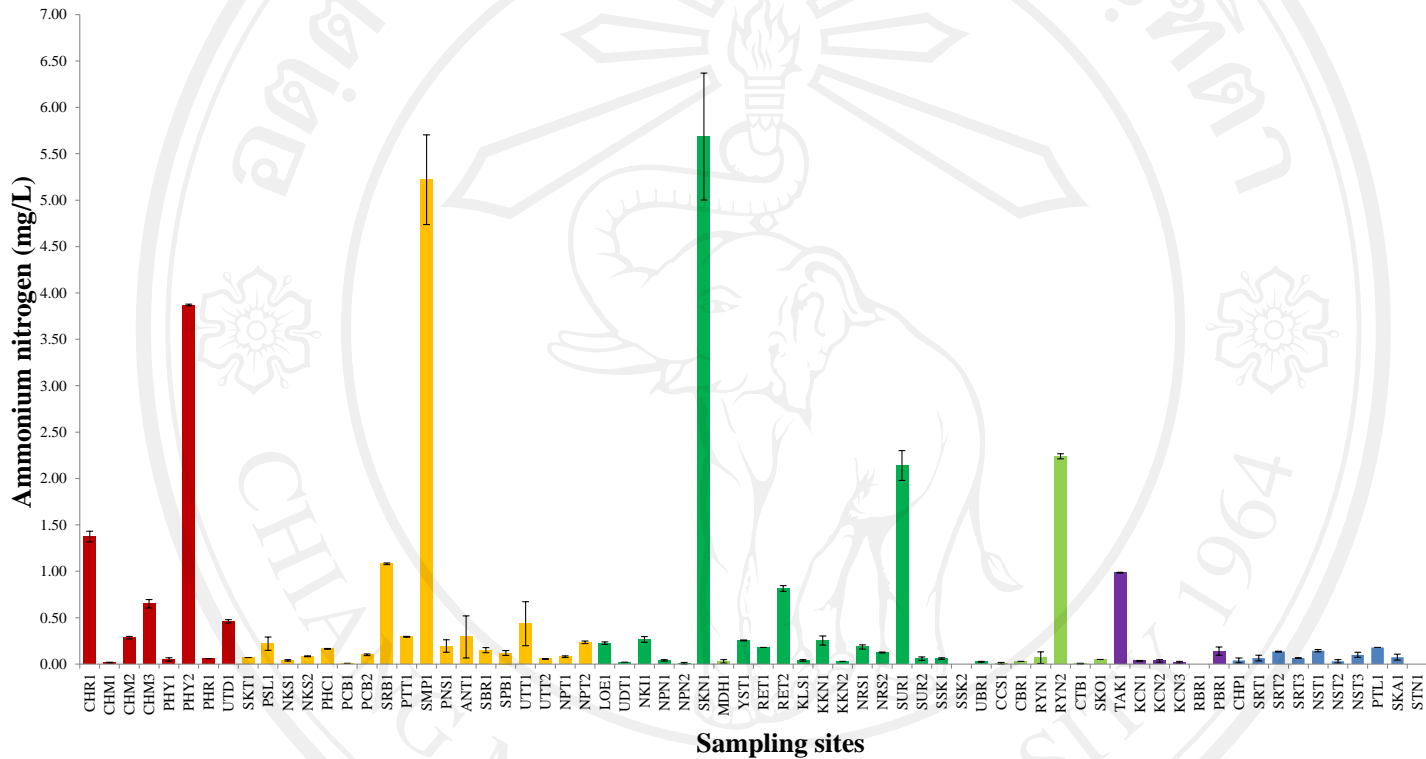


Figure 21 Biochemical oxygen demand of water at 68 sampling sites



■ Northern part
 ■ Central part
 ■ Northeastern part
 ■ Eastern part
 ■ Western part
 ■ Southern part

Figure 22 Ammonium nitrogen of water at 68 sampling sites

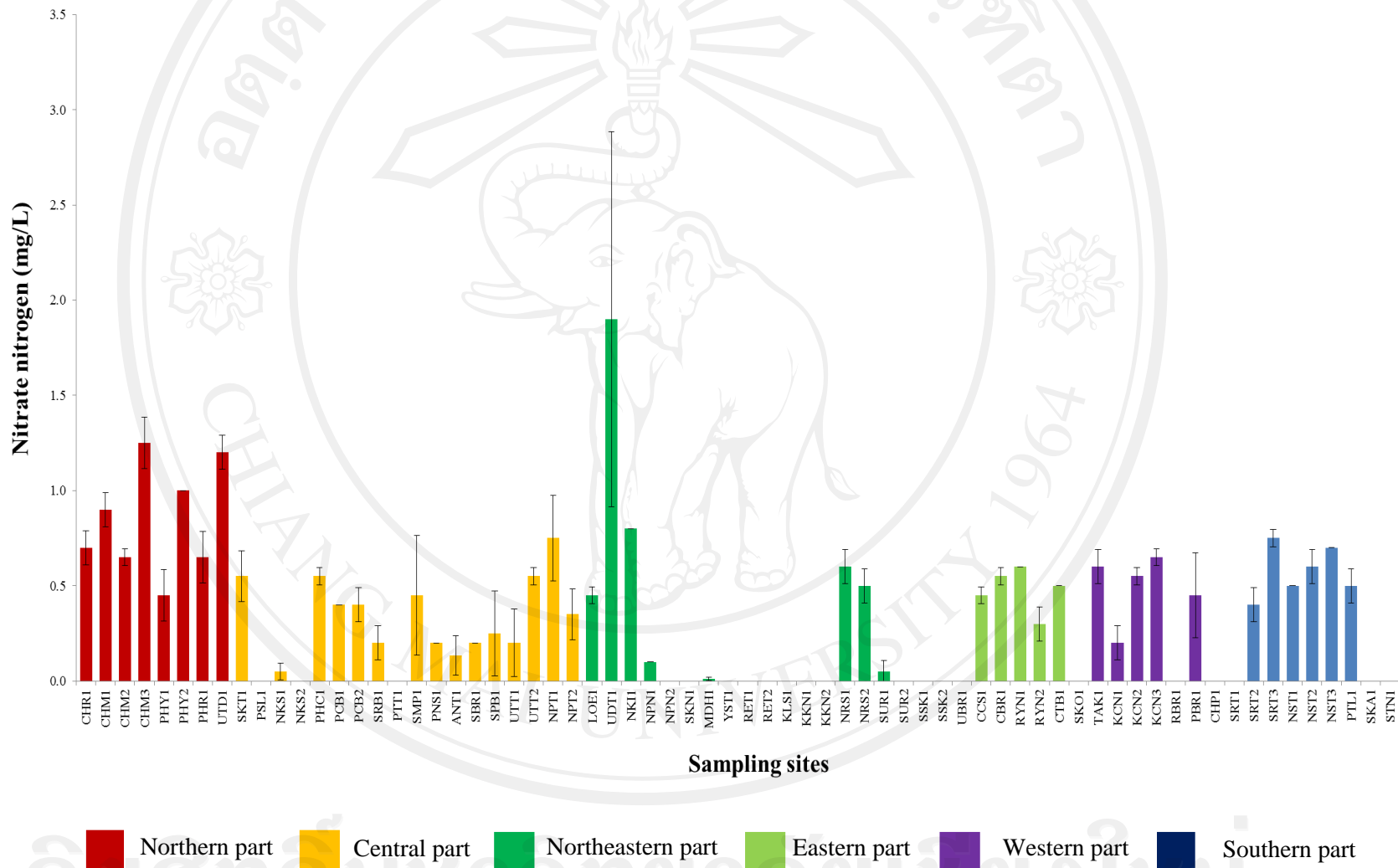


Figure 23 Nitrate nitrogen of water at 68 sampling sites

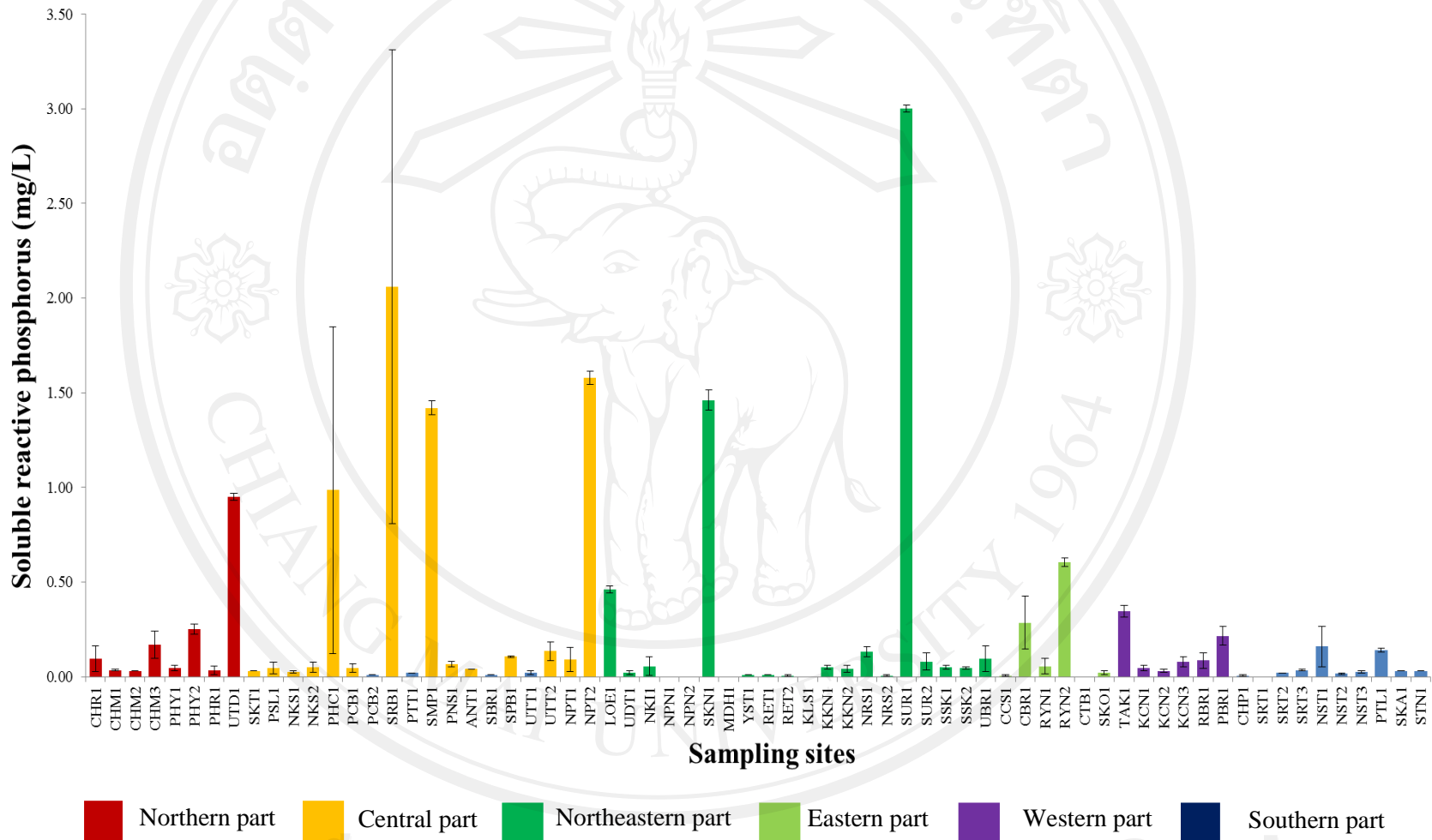


Figure 24 Soluble reactive phosphorus of water at 68 sampling sites

ลิขสิทธิ์ © by Chiang Mai University
All rights reserved

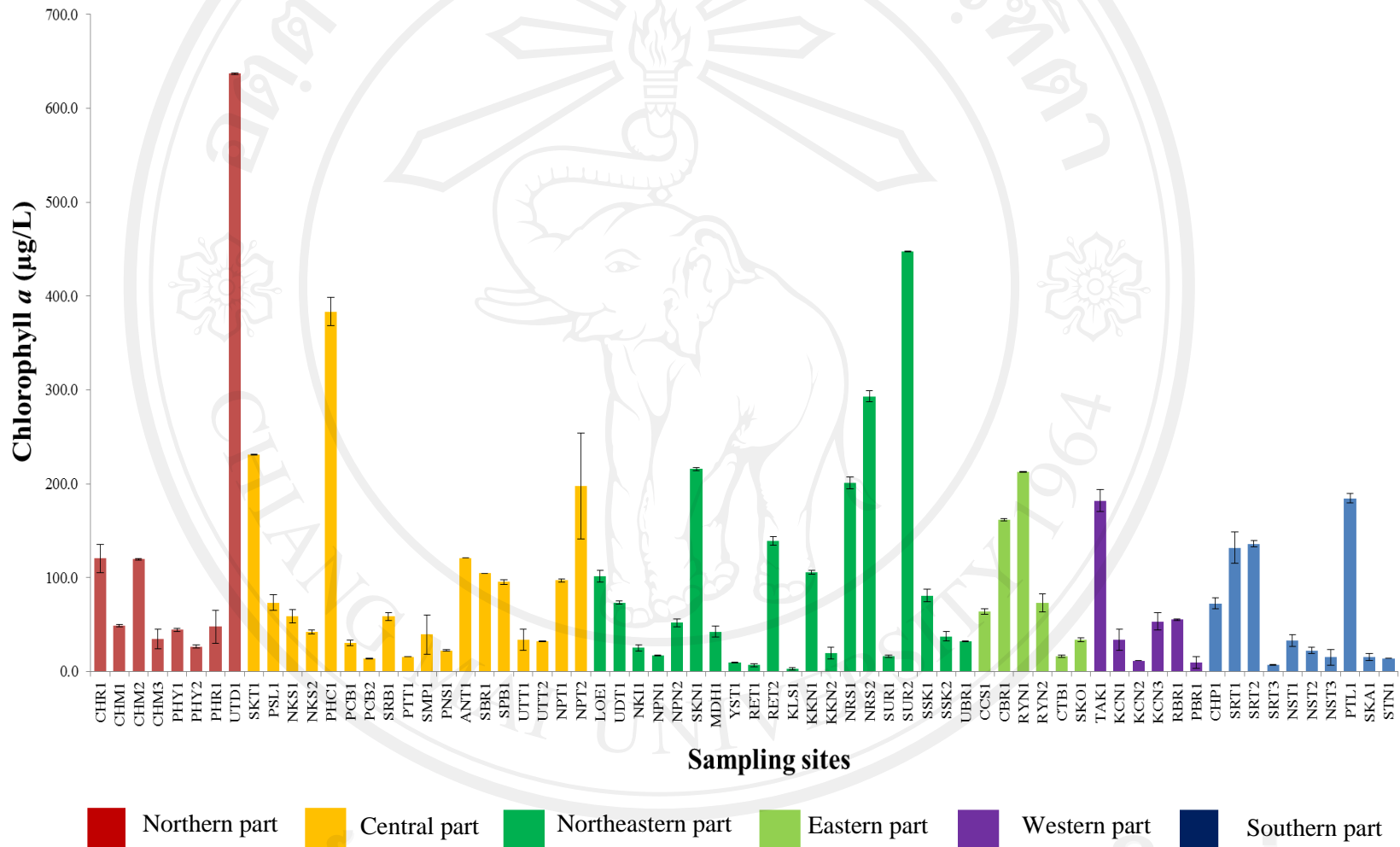
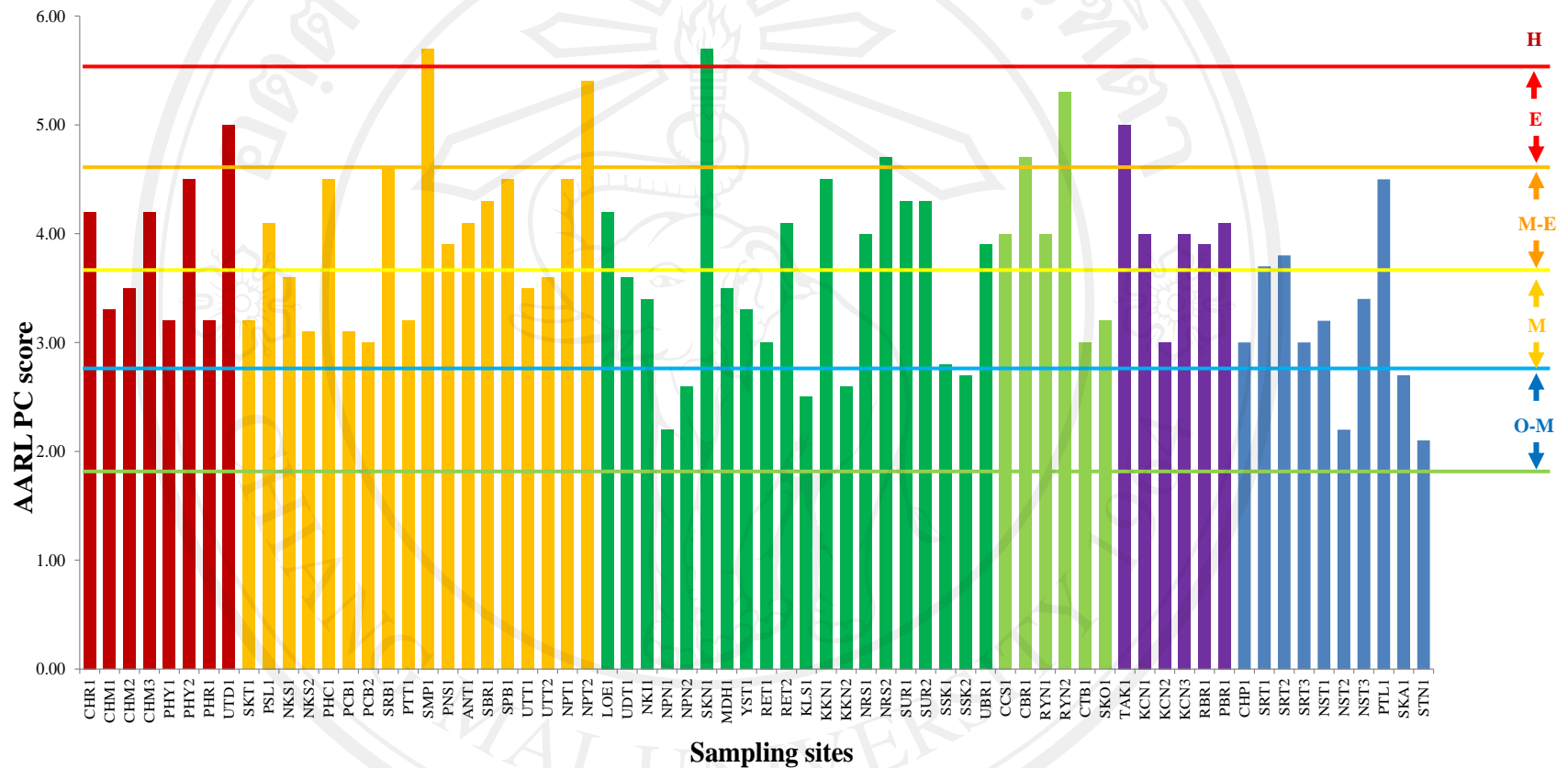


Figure 25 Chlorophyll *a* of water at 68 sampling sites

ลิขสิทธิ์มหาวิทยาลัยเชียงใหม่
 Copyright © by Chiang Mai University
 All rights reserved



O-M = Oligo-mesotrophic status
M = Mesotrophic status
M-E = Meso-eutrophic status
E = Eutrophic status
H = Hypereutrophic status

Figure 26 Trophic status of water at 68 sampling sites by using AARL-PC Score

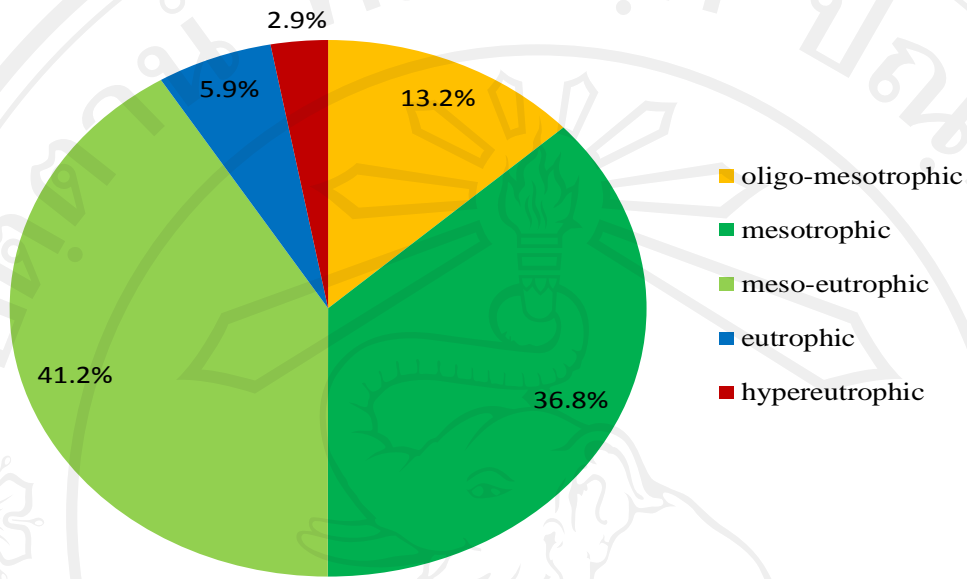


Figure 27 Trophic status proportion at 68 sampling sites

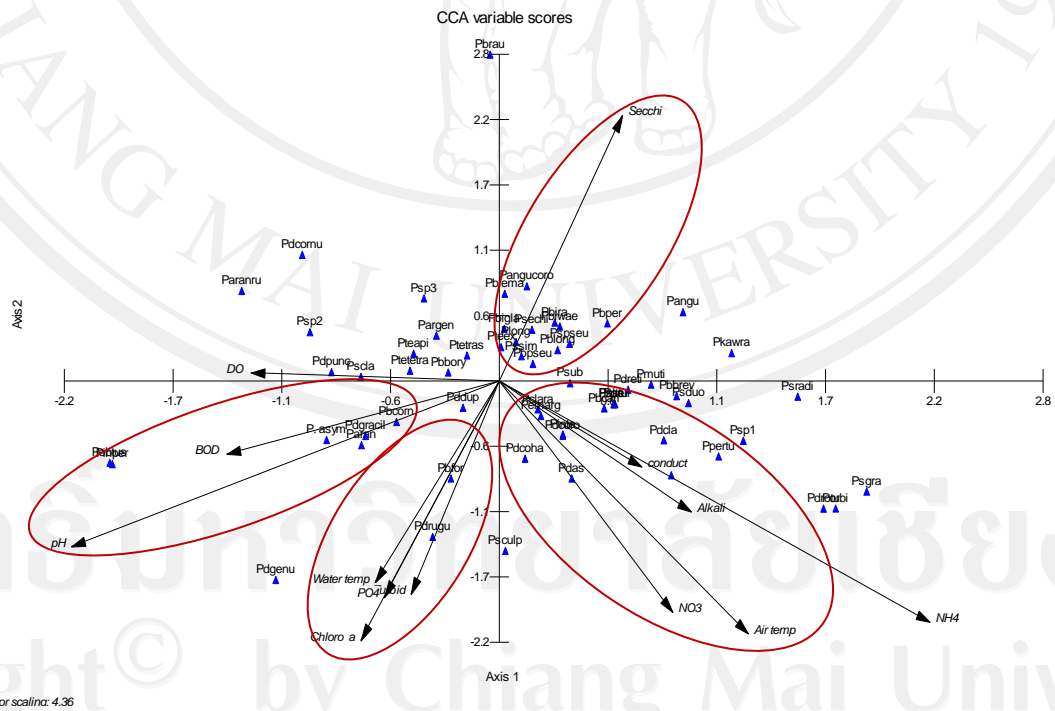


Figure 28 Canonical Correspondence Analysis (CCA) of the physic-chemical parameters and *Pediastrum* spp.

4.6 Isolation and Cultivation of *Pediastrum* spp.

The dominant species of *Pediastrum* i.e. *P. boryanum*, *P. duplex*, *P. simplex* and *P. tetras* were selected for optimal study of media, pH and temperature.

4.6.1 Effect of media

Comparison between of the growth of the four dominant species of *Pediastrum* in 3 media: Jaworski's medium (JM), algal medium (AM) and bold basal medium (BBM) and the cell density was determined spectrophotometrically at a wavelength of 665 nm and cell counts by whole counts method. It was shown that the growth of *P. boryanum* was highest in BBM with OD₆₆₅ at 1.17 and cell number at 66×10^6 cell/mL on Day 12 followed by the growth in JM and AM respectively. *P. duplex*, *P. simplex* and *P. tetras* were found to grow best in JM with OD₆₆₅ at 0.87 0.80 and 0.74 respectively and cell number at 94×10^6 , 78×10^6 and 45×10^6 cell/mL respectively. (Figures 29 and 30). The biomass productivity of the four species was studied using AM, BBM and JM. There was no significant difference ($p < 0.05$) between the productivity in BBM and JM but significant difference ($p < 0.05$) between BBM and AM and between JM and AM (Figure 30).

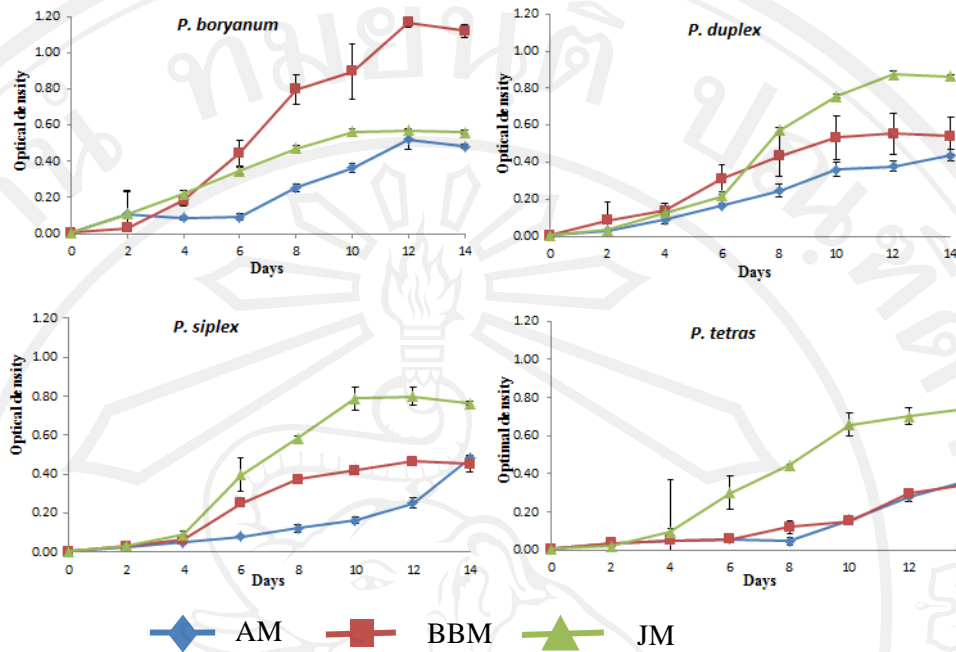


Figure 29 Growth (optical density) of *P. boryanum* in BBM; *P. duplex*, *P. simplex* and *P. tetras* in JM

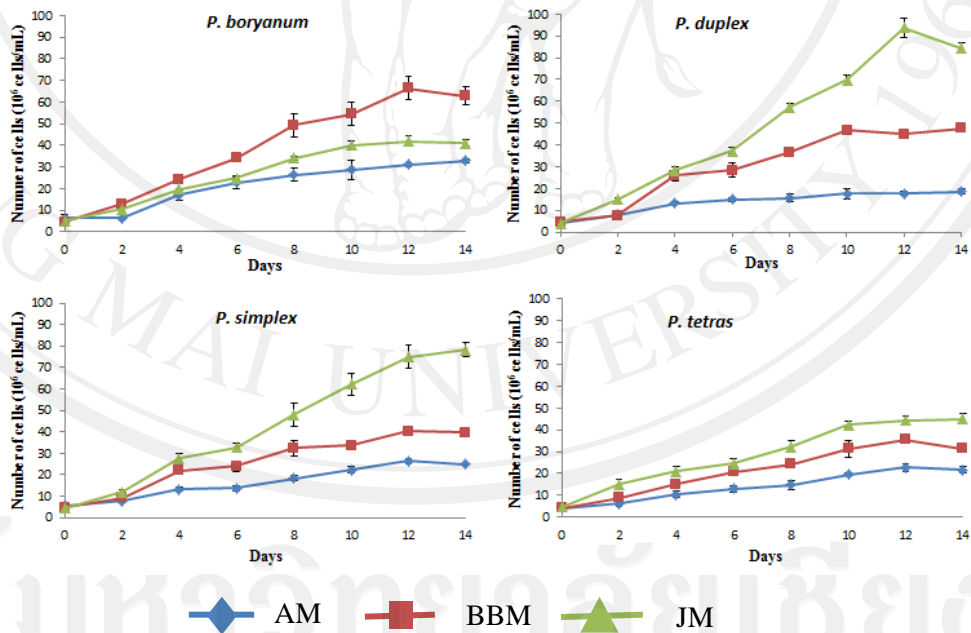


Figure 30 Growth (cell number) of *P. boryanum* in BBM; *P. duplex*, *P. simplex* and *P. tetras* in JM

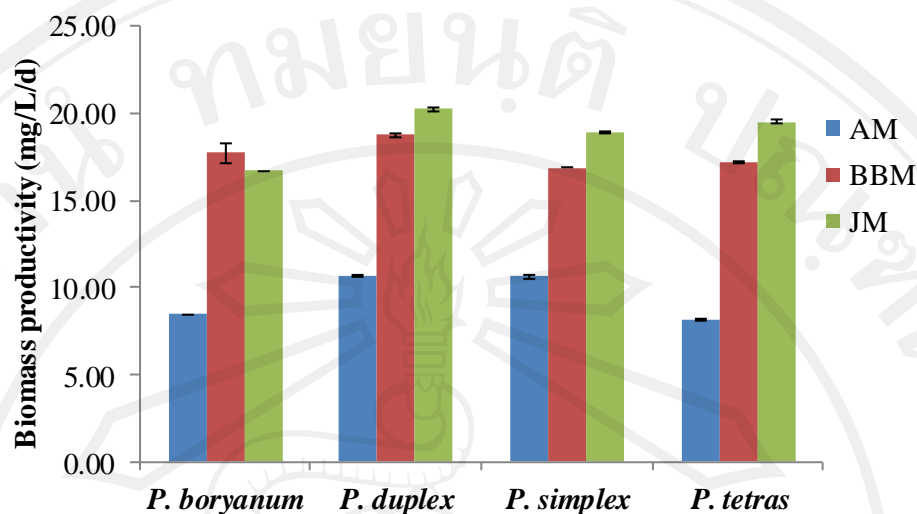


Figure 31 Biomass productivity as dry weight (mg/L/d) of *P. boryanum* in BBM; *P. duplex*, *P. simplex* and *P. tetras* in JM

4.6.2 Effect of pH

The dominant species of *Pediastrum* were cultivated at different pH: 6.5, 7.0, 7.5 and 8.0. *P. boryanum* was found to grow best at pH 7.5 in BBM medium with highest OD₆₆₅ at 0.903 and cell number at 78×10^6 cell/mL. *P. duplex*, *P. simplex* and *P. tetras* exhibited highest growth at pH 8.0 in JM and highest OD₆₆₅ at 0.897, 0.715 and 0.870 and cell number at 87×10^6 , 74×10^6 and 76×10^6 cell/mL respectively (Figures 32 and 33). The biomass productivity of *P. boryanum* in BBM was studied at pH 6.5, 7.0, 7.5 and 8.0. There was significant difference ($p < 0.05$) in the productivity of *P. boryanum* between pH 7.5 and 6.5, 7.0, 8.0 but no significant difference ($p < 0.05$) at pH 6.5, 7.0 and 8.0. The biomass productivity of *P. duplex*, *P. simplex* and *P. tetras* in JM was studied at pH 6.5, 7.0, 7.5 and 8.0. There was significantly difference ($p < 0.05$) in the productivity between pH 8.0 and 6.5, 7.0, 7.5 but no significant difference ($p < 0.05$) between pH 6.5, 7.0, 7.5. (Figure 34).

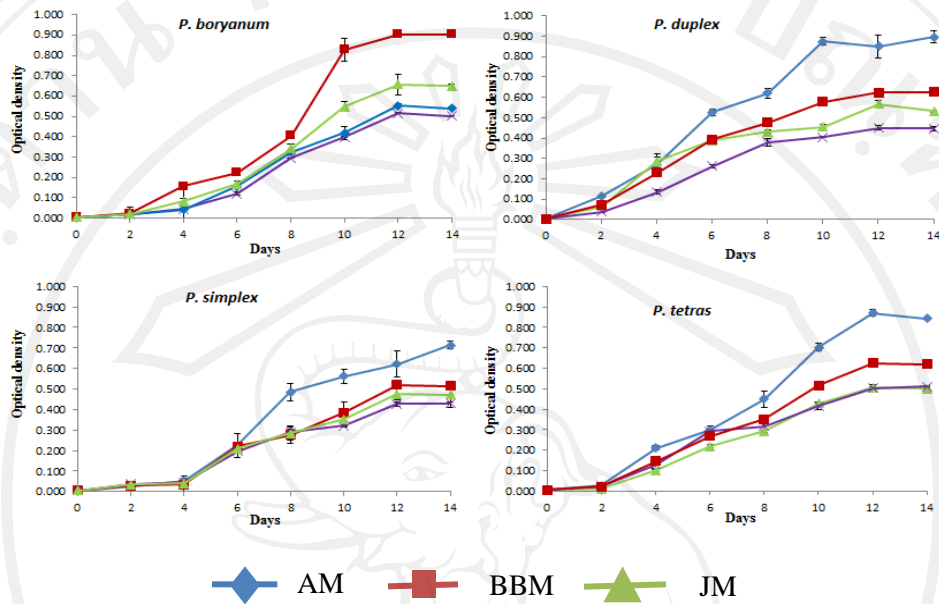


Figure 32 Growth (optical density) of *P. boryanum* in BBM; *P. duplex*, *P. simplex* and *P. tetras* in JM at different pH

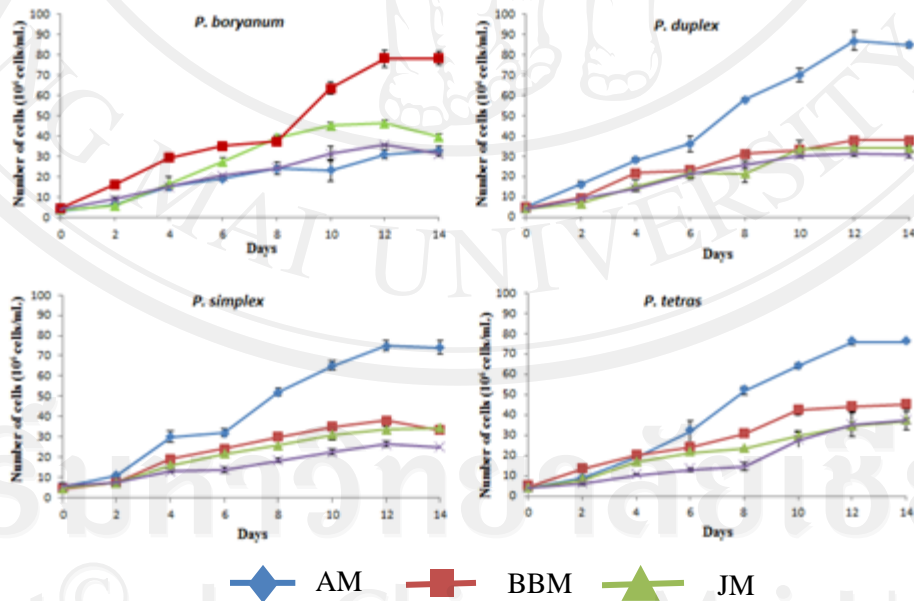


Figure 33 Growth (cell number) of *P. boryanum* in BBM; *P. duplex*, *P. simplex* and *P. tetras* in JM at different pH

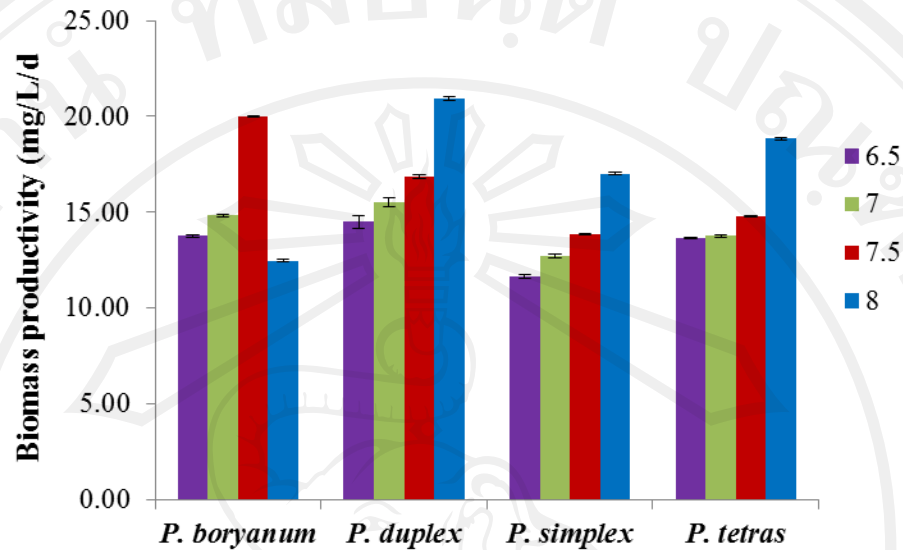


Figure 34 Biomass productivity as dry weight (mg/L/d) of *P. boryanum* in BBM; *P. duplex*, *P. simplex* and *P. tetras* in JM at different pH

4.6.3 Effect of temperature

The dominant species of *Pediastrum* were cultivated at 25 °C and room temperature. The minimum temperature was 26.0-28.5 °C and maximum temperature was 29.0-33.0 °C. *P. boryanum* were found to exhibit highest growth in BBM at pH 7.5 at room temperature with OD₆₆₅ at 0.80 and cell number at 71×10⁶ cell/mL, *P. duplex*, *P. simplex* and *P. tetras* were found to exhibit highest growth in JM at pH 7.5 at room temperature with OD₆₆₅ at 0.87, 0.70 and 0.77 and highest cell number at 86×10⁶, 74×10⁶ and 77×10⁶ cell/mL respectively (Figures 35 and 36).

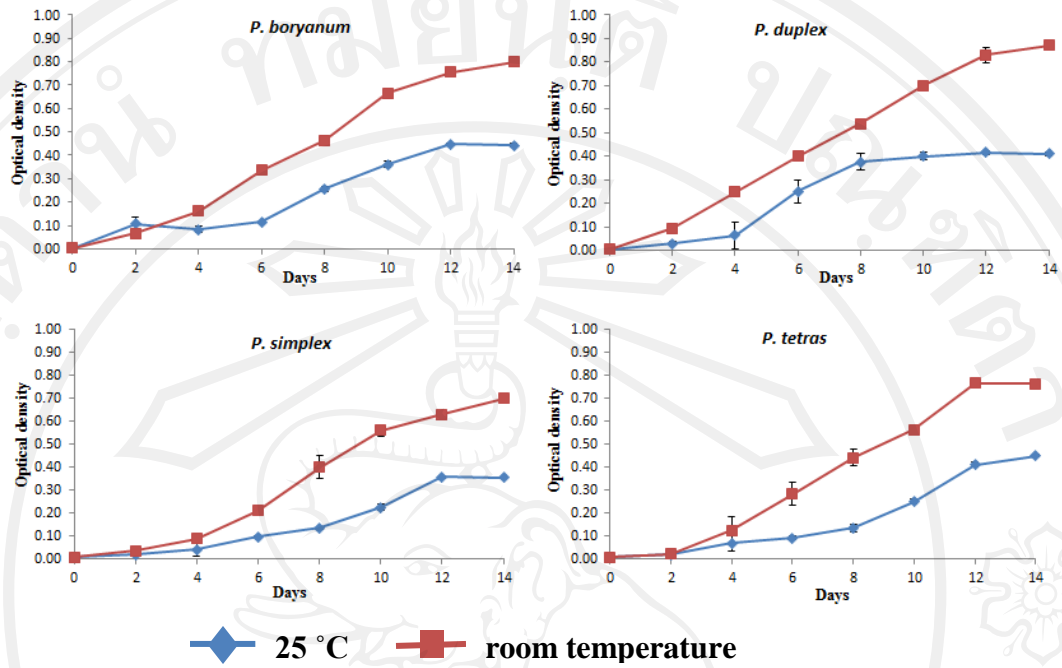


Figure 35 Growth (optical density) of *P. boryanum* in BBM; *P. duplex*, *P. simplex* and *P. tetras* in JM at different temperatures

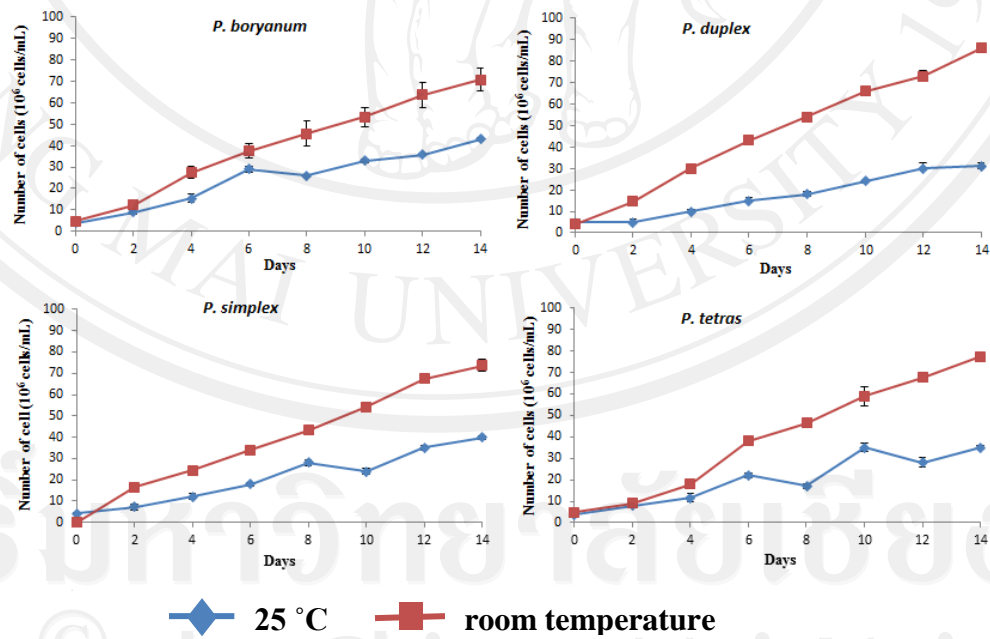


Figure 36 Growth (cell number) of *P. boryanum* in BBM; *P. duplex*, *P. simplex* and *P. tetras* in JM at different temperatures

4.7 Nutritional value of dominant species of *Pediastrum* spp.

At the end of cultivation, the biomass of the dominant species of *Pediastrum* were collected for nutritional analysis. Proximate composition of dominant species of *Pediastrum* is shown in Table 5. Protein contents of *P. boryanum*, *P. duplex*, *P. simplex* and *P. tetras* were 30.17, 36.45, 35.93 and 30.44 g/100g respectively, carbohydrate contents were 43.49, 32.88, 34.41 and 43.86 g/100g respectively, fat contents were 7.50, 14.06, 13.56 and 10.29 g/100 g respectively, ash contents were 8.80, 8.74, 8.73 and 6.50 g/100g respectively and moisture contents were 10.04, 7.84, 7.73 and 8.91 g/100 g respectively.

Table 5 Proximate composition of dominant species of *Pediastrum* spp.

Taxa	Protein g/100g	Carbohydrate g/100g	Fat g/100g	Ash g/100g	Moisture g/100g
<i>P. boryanum</i>	30.17	43.49	7.50	8.80	10.04
<i>P. duplex</i>	36.45	32.88	14.06	8.74	7.87
<i>P. simplex</i>	35.93	34.41	13.56	8.73	7.73
<i>P. tetras</i>	30.44	43.86	10.29	6.50	8.91

4.8 Phylogenetic analysis of the 26S rDNA and rbcL sequence

A total of 22 taxa were isolated for molecular analysis (Table 6). Phylogenetic relationships were inferred using Maximum Likelihood (ML) method. These phylogenetic trees were calculated based on 1335 bp for each sample. The data from the 26S rDNA and rbcL were analyzed separately as shown in Figures 36 and 37.

4.8.1 Phylogenetic analysis of the 26S rDNA

M25 showed closely relationship with *Pseudopediastrum boryanum* group and M8 and M9 reveal a close relationship with *Pediastrum duplex* var. *gracillimum*. M16 is closely related to *Pediastrum simplex* group in the 26S rDNA. *Pediastrum simplex* is not supported as monophyletic in the 26S rDNA which was separated in two groups (Figure 36). Group I includes M26 (*P. simplex* var. *pseudogrsbrum*) and M28 (*P. biwae*, the synonym is *Pediastrum simplex* var. *biwaense*). Group II includes M32 (*P. simplex* var. *echinulatum*) and M33 (*P. simplex* var. *sturmii*). M5 reveal a close relationship with *Parapediastrum biradiatum* and these clade is sister to *Sorastrum* group. M18 and M20 reveals a close relationship with *Pediastrum tetras*.

4.8.2 Phylogenetic analysis of the rbcL sequence

M2 is closely related to *Pediastrum duplex* SL0405MN which was supported as >50 bootstarp and M13 is closely related to *Pediastrum duplex* CRO501a which was strongly supported as >90 bootstarp. M4, M10, M3 and M15 are closely related to *Pediastrum duplex* UTAX LB1364 *Pediastrum duplex* UBO404 which was supported as >50 bootstarp. M25 is closely related to *Pseudopediastrum boryanum* CL0201VA. M8, M9 and M11 reveal a close relationship to *Pediastrum duplex* var. *gracillimum* AC0392. M30 and M28 *Pediastrum simplex* var. *pseudogrsbrum* AC011043. M16 (*Pediastrum asymmetricum*) is closely related to *Pediastrum simplex* group. M32, M33, M31 and M27 are closely related to *Monactinus simplex* UTEXLB1601 and *Pediastrum simplex* f. *stumii* AC011041. M18 is closely related to *Stauridium tetras* UTEX 38 which was

supported as >50. M5 is closely related to *Parapediastrium biradiatum* UTEX 37 which was strong supported as >90. (Figure 37)

Table 6 Taxa of *Pediastrum* spp. for studied phylogenetic analysis

code	Taxa	Study site
M2	<i>P. duplex</i>	CHM1
M3	<i>P. duplex</i>	CHM2
M4	<i>P. duplex</i>	CHM3
M5	<i>P. biradiatum</i>	CHM3
M8	<i>P. duplex</i> var. <i>gracillimum</i>	UTD1
M9	<i>P. duplex</i> var. <i>gracillimum</i>	PTL1
M10	<i>P. duplex</i>	PTL1
M11	<i>P. duplex</i> var. <i>gracillimum</i>	NKS1
M12	<i>P. duplex</i>	PHY2
M13	<i>P. duplex</i>	UTD1
M15	<i>P. duplex</i>	NKS1
M16	<i>P. asymmetricum</i>	PCB1
M18	<i>P. tetras</i>	CHM1
M20	<i>P. tetras</i>	CHM3
M25	<i>P. boryanum</i>	CHM3
M26	<i>P. simplex</i> var. <i>pseudogrbrum</i>	CHM3
M27	<i>P. simplex</i> var. <i>simplex</i>	SRT2
M28	<i>P. biwae</i>	CHM3
M30	<i>P. simplex</i> var. <i>simplex</i>	CHM3
M31	<i>P. simplex</i> var. <i>echinulatum</i>	PHY1
M32	<i>P. simplex</i> var. <i>echinulatum</i>	KLS1
M33	<i>P. simplex</i> var. <i>sturmii</i>	CHM3

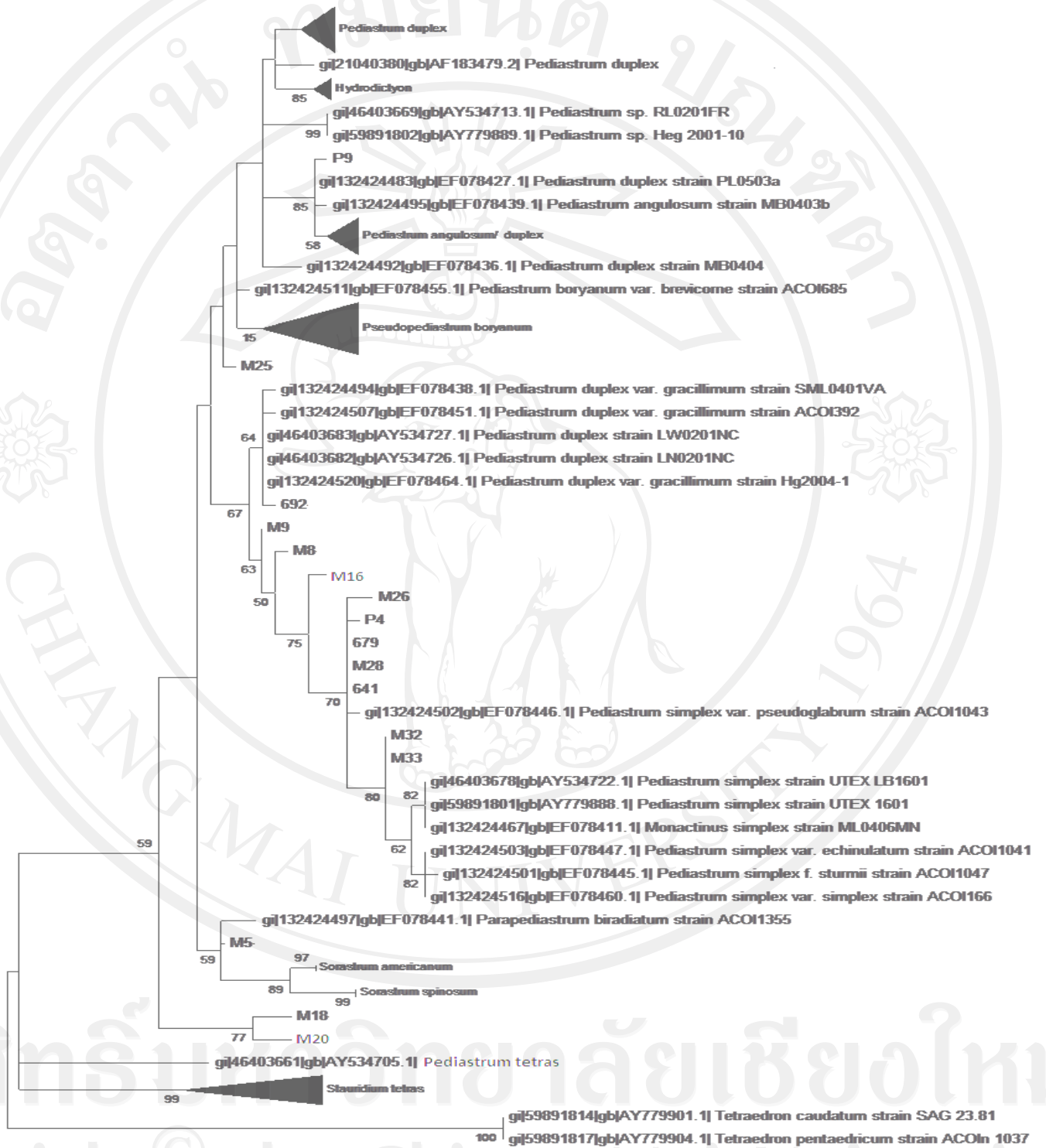


Figure 37 Maximum likelihood phylogenetic tree estimated from analysis of 26S rDNA sequence data, under the GTR + G + I model of evolution. Nodal support is shown on branches with Bootstrap branch support (BS) values >50%

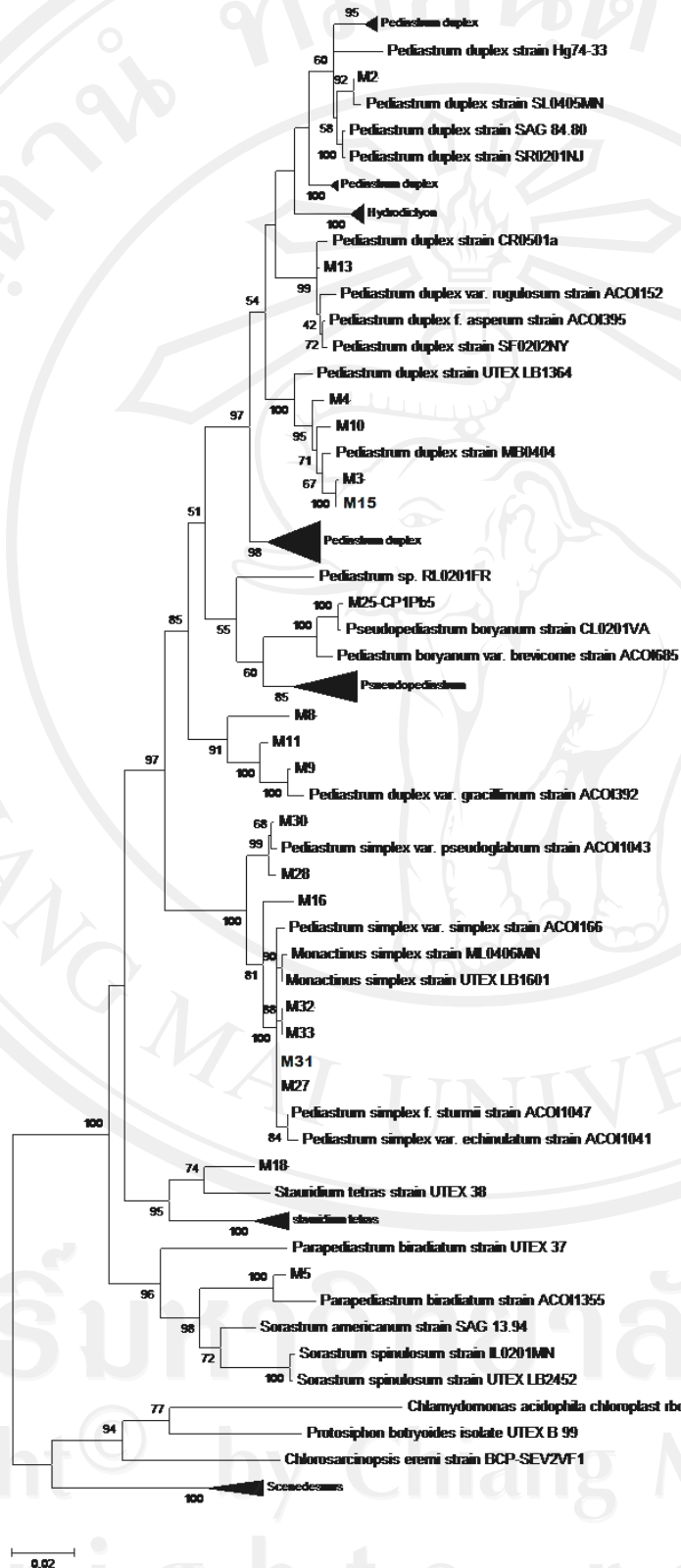


Figure 38 Maximum likelihood phylogenetic tree estimated from an analysis of *rbcL* sequence data, under the GTR + G + I model of evolution. Nodal support is shown on branches with Bootstrap branch support (BS) values >50%